The Journal of Immunology

Invariant NKT Cell Activation Induces Late Preterm Birth That Is Attenuated by Rosiglitazone

Derek St. Louis, Roberto Romero, Olesya Plazyo, Marcia Arenas-Hernandez, Bogdan Panaitescu, Yi Xu, Tatjana Milovic, Zhonghui Xu, Gaurav Bhatti, Qing-Sheng Mi, Sascha Drewlo, Adi L. Tarca, Sonia S. Hassan and Nardhy Gomez-Lopez

J Immunol 2016; 196:1044-1059; Prepublished online 6 January 2016;
doi: 10.4049/jimmunol.1501962
http://www.jimmunol.org/content/196/3/1044

The Journal of Immunology is published twice each month by
The American Association of Immunologists, Inc.,
1451 Rockville Pike, Suite 650, Rockville, MD 20852

Print ISSN: 0022-1767 Online ISSN: 1550-6606.

Invariant NKT Cell Activation Induces Late Preterm Birth That Is Attenuated by Rosiglitazone

Derek St. Louis,[*,†,1] Roberto Romero,[†,‡,§,¶,1] Olesya Plazyo,[*,†,1] Marcia Arenas-Hernandez,[*,†] Bogdan Panaitescu,[‖] Yi Xu,[†] Tatjana Milovic,[*] Zhonghui Xu,[*,†] Gaurav Bhatti,[*,†] Qing-Sheng Mi,[#,,††] Sascha Drewlo,[*] Adi L. Tarca,[*,†] Sonia S. Hassan,[*,†] and Nardhy Gomez-Lopez[*,†,††]**

Preterm birth (PTB) is the leading cause of neonatal morbidity and mortality worldwide. Although intra-amniotic infection is a recognized cause of spontaneous preterm labor, the noninfection-related etiologies are poorly understood. In this article, we demonstrated that the expansion of activated CD1d-restricted invariant NKT (iNKT) cells in the third trimester by administration of α-galactosylceramide (α-GalCer) induced late PTB and neonatal mortality. In vivo imaging revealed that fetuses from mice that underwent α-GalCer–induced late PTB had bradycardia and died shortly after delivery. Yet, administration of α-GalCer in the second trimester did not cause pregnancy loss. Peroxisome proliferator–activated receptor (PPAR)γ activation, through rosiglitazone treatment, reduced the rate of α-GalCer–induced late PTB and improved neonatal survival. Administration of α-GalCer in the third trimester suppressed PPARγ activation, as shown by the downregulation of *Fabp4* and *Fatp4* in myometrial and decidual tissues, respectively; this suppression was rescued by rosiglitazone treatment. Administration of α-GalCer in the third trimester induced an increase in the activation of conventional $CD4^+$ T cells in myometrial tissues and the infiltration of activated macrophages, neutrophils, and mature dendritic cells to myometrial and/or decidual tissues. All of these effects were blunted after rosiglitazone treatment. Administration of α-GalCer also upregulated the expression of inflammatory genes at the maternal–fetal interface and systemically, and rosiglitazone treatment partially attenuated these responses. Finally, an increased infiltration of activated iNKT-like cells in human decidual tissues is associated with noninfection-related preterm labor/birth. Collectively, these results demonstrate that iNKT cell activation in vivo leads to late PTB by initiating innate and adaptive immune responses and suggest that the PPARγ pathway has potential as a target for prevention of this syndrome. ***The Journal of Immunology*****, 2016, 196: 1044–1059.**

Preterm birth (PTB) refers to the delivery of a live baby before the 37th week of gestation, and it is the leading cause of neonatal morbidity and mortality worldwide (1). In 2013, 11.39% of births in the United States were preterm (2). Preterm neonates are at an increased risk for short- and long-term morbidity, and prematurity represents a substantial burden for society (3–6). Approximately 72% of all PTBs are diagnosed as late preterm (34 to <37 wk) (7, 8), and two thirds of all PTBs occur after spontaneous preterm labor (9). Therefore, we focused our attention on the elucidation of those mechanisms that lead to spontaneous late preterm labor/birth and the development of therapies to prevent this syndrome.

Inflammation is implicated in the pathological process of spontaneous preterm labor (10–38). Pathological inflammation can result from the activation of innate immunity (39–47) by microorganisms (24, 48) or endogenous danger signals derived from necrosis or cellular stress (44, 49–52) termed damage-associated molecular pattern molecules (53) or alarmins (54). The inflammatory process initiated by alarmins is known as sterile inflammation (55). The term sterile intra-amniotic inflammation refers to an inflammatory process in which microorganisms cannot be detected in the amniotic cavity (44, 49–52, 56). Sterile intra-amniotic inflammation is more common than microbial-associated intra-amniotic inflammation in patients with spontaneous preterm labor

*Department of Obstetrics and Gynecology, Wayne State University School of Medicine, Detroit, MI 48201; [†]Perinatology Research Branch, Program for Perinatal Research and Obstetrics, Division of Intramural Research, Eunice Kennedy Shriver National Institute of Child Health and Human Development, National Institutes of Health/U.S. Department of Health and Human Services, Bethesda, MD 20892 and Detroit, MI 48201; [‡]Department of Obstetrics and Gynecology, University of Michigan, Ann Arbor, MI 48109; [§]Department of Epidemiology and Biostatistics, Michigan State University, East Lansing, MI 48825; [¶]Center for Molecular Medicine and Genetics, Wayne State University, Detroit, MI 48201; [‖]Department of Pediatrics, Neonatology Division, Wayne State University School of Medicine, Detroit, MI 48201; [#]Immunology Program, Henry Ford Health System, Detroit, MI 48202; **Department of Dermatology, Henry Ford Health System, Detroit, MI 48202; and [††]Department of Immunology and Microbiology, Wayne State University School of Medicine, Detroit, MI 48201

[1]D.S.L., R.R., and O.P. contributed equally to this work.

ORCIDs: 0000-0002-4448-5121 (R.R.); 0000-0002-1178-6112 (M.A.-H.); 0000-0001-5917-9912 (T.M.); 0000-0002-1411-6827 (Q.-S.M.); 0000-0002-9281-126X (A.L.T.).

Received for publication September 2, 2015. Accepted for publication November 24, 2015.

This work was supported by the Wayne State University Perinatal Initiative in Maternal, Perinatal, and Child Health, as well as by the Perinatology Research Branch, Division of Intramural Research, Eunice Kennedy Shriver National Institute of Child Health and Human Development, National Institutes of Health, U.S. Department of Health and Human Services. Q.-S.M. was supported by National Institutes of Health/National Institute of Allergy and Infectious Diseases Grant 1R56AI119041.

Address correspondence and reprint requests to Dr. Nardhy Gomez-Lopez, Department of Obstetrics and Gynecology, Wayne State University School of Medicine, C.S. Mott Center for Human Growth and Development, 275 E. Hancock Street, Detroit, MI 48201. E-mail addresses: nardhy.gomez-lopez@wayne.edu and ngomezlo@med.wayne.edu

The online version of this article contains supplemental material.

Abbreviations used in this article: B6, C57BL/6J; DC, dendritic cell; dpc, day post coitum; Fabp4, fatty acid binding protein 4; Fatp4, fatty acid transport protein 4; α-GalCer, α-galactosylceramide; iNKT, invariant NKT; PPARγ, peroxisome proliferator–activated receptor γ; PTB, preterm birth; PTL, preterm with labor; PTNL, preterm without labor; qRT-PCR, quantitative real-time PCR; TIL, term with labor; TNL, term without labor; Treg, regulatory T cell; ULN, uterine lymph node.

(30, 57). Indeed, administration of alarmins, such as IL-1α (58) or HMGB1 (59), induces preterm labor/birth. In addition, IL-33, a classic alarmin (60), is expressed in decidual tissues and upregulated in acute chorioamnionitis (61), a placental lesion associated with preterm labor (62). Recently, it was demonstrated that IL-33 is a potent activator of invariant NKT (iNKT) cells (63, 64). Therefore, we hypothesized that activation of iNKT cells, immune cells that can be targeted by alarmins in the context of sterile inflammation, could participate in the immune mechanisms that lead to noninfection-related preterm labor/birth.

iNKT cell activation causes the initiation of signaling pathways (e.g., the NF-κB pathway) leading to the production of Th1 and Th2 cytokines and chemokines (65–70), which, in turn, induce a massive immune response mediated by innate and adaptive immune cells (71). Hence, we hypothesized that iNKT cell activation via α-galactosylceramide (α-GalCer), a high-affinity iNKT ligand (72, 73), would initiate innate and adaptive immune responses at the maternal–fetal interface, promoting pathological inflammation and leading to spontaneous preterm labor/birth. In addition, we proposed that suppression of this inflammatory response would prevent PTB induced by iNKT cell activation. In search of an anti-inflammatory drug to prevent PTB, we evaluated rosiglitazone, a selective peroxisome proliferator–activated receptor (PPAR)γ agonist (74). Rosiglitazone causes activation of the PPARγ pathway, which, in turn, suppresses gene transcription by interfering with signal-transduction pathways, such as the NF-κB, STAT, and AP-1 pathways (75–77). PPARγ activation was suggested as a therapeutic intervention for preventing PTB (78) because treatment with 15-deoxy-$\Delta^{12,14}$-PG J_2 compound, a PPARγ agonist (79, 80), delays endotoxin-induced PTB (81). However, whether rosiglitazone blunts the inflammatory response induced by iNKT cell activation has not been investigated.

Using a murine model, our investigations demonstrate for the first time, to our knowledge, that administration of α-GalCer in the third trimester leads to late PTB, which is prevented following PPARγ activation by treatment with rosiglitazone. In addition, we describe that PPARγ activation regulates immune mechanisms locally, at the maternal–fetal interface, and systemically to attenuate α-GalCer–induced late PTB. Finally, we broaden the significance of our findings by demonstrating an increase in activated iNKT-like cells in decidual tissue from women who underwent spontaneous preterm labor/birth.

Materials and Methods

Animals

C57BL/6J (B6) mice were bred in the animal care facility at the C.S. Mott Center for Human Growth and Development at Wayne State University and housed under a circadian cycle (light/dark = 12:12 h). Eight- to twelve-week-old females were mated with male mice of proven fertility. Female mice were examined daily between 8:00 and 9:00 AM for the presence of a vaginal plug, which denoted 0.5 days post coitum (dpc). Upon observation of vaginal plugs, female mice were separated from the males and housed in other cages. A weight gain ≥ 2 g confirmed pregnancy at 12.5 dpc. Procedures were approved by the Institutional Animal Care and Use Committee at Wayne State University (Protocol No. A-09-08-12).

α-GalCer–induced late PTB model

Pregnant B6 mice were injected i.v. with 1, 2, 3, or 4 μg α-GalCer (KRN7000; Funakoshi, Tokyo, Japan; $n = 3$ for 1, 3, or 4 μg; $n = 20$ for 2 μg) that had been dissolved in 50 μl 4% DMSO (Sigma-Aldrich, St. Louis, MO) or with 50 μl 4% DMSO alone (referred to throughout the manuscript as DMSO) as a control ($n = 19$) at 16.5 dpc (third trimester). Following injection, pregnant mice were monitored using a video camera with infrared light (Sony, Tokyo, Japan) until delivery. A second group of mice was injected i.v. with either 2 μg α-GalCer or DMSO at 10.5 dpc ($n = 5$ each; second trimester), and inspection of resorption sites was performed at 14.5 dpc. A third group of mice was injected i.v. with 2 μg α-GalCer at 10.5 dpc ($n = 3$) and monitored during delivery; photographs of the neonates were taken at 1 and 2 d after birth using a camera (Sony).

Video monitoring, pup mortality, and neonatal weight

Video monitoring allowed for determination of gestational age and rate of pup mortality. Gestational age was calculated from the presence of the vaginal plug (0.5 dpc) until the observation of the first pup in the cage bedding. The rate of pup mortality for each litter was defined as the proportion of born pups found dead among the total litter size. Late PTB was defined as delivery between 18.0 and 18.5 dpc. Neonatal survival and weight were recorded 1 wk postpartum.

In vivo imaging by ultrasound

On the morning of 16.5 dpc, pregnant B6 mice were anesthetized by inhalation of 2–3% isoflurane (Aerrane; Baxter Healthcare, Deerfield, IL) and 1–2 l/min oxygen in an induction chamber. Using Doppler ultrasound, the fetal heart rate and umbilical artery hemodynamic parameters were recorded (VisualSonics, Toronto, ON, Canada). Following ultrasound, dams were placed under a heat lamp for recovery, which occurred 10–20 min after heating. On the same day at noon, dams were injected with 2 μg α-GalCer or DMSO, as described previously ($n = 3$ each). On the afternoon of 17.5 dpc (just prior to late PTB in those mice injected with α-GalCer), a second ultrasound was performed, and the same hemodynamic parameters were evaluated.

Video monitoring by infrared thermography

Pregnant B6 mice were injected i.v. with 2 μg α-GalCer at 16.5 dpc ($n = 3$). Immediately after late preterm delivery, the body temperature of the newborns was monitored using a thermal infrared camera (FLIR e50; FLIR Systems, Wilsonville, OR). Temperature readings were recorded at 15 and 30 s, as well as at 1, 2, 3.5, 5.5, and 8 min after birth. A newborn that maintained a constant body temperature was considered a viable pup, whereas a newborn whose body temperature gradually decreased to the level of room temperature was qualified as a dead pup; viable and dead pups were also confirmed by visual analysis.

Fetal and placental weights

Pregnant B6 mice were injected i.v. with 2 μg α-GalCer ($n = 8$) or DMSO ($n = 6$) at 16.5 dpc. Six hours after injection, dams were euthanized, and placental and fetal weights were measured using a scale (DIA-20; American Weight Scales, Norcross, GA).

Rosiglitazone treatment of α-GalCer–induced late PTB

Pregnant B6 mice were injected i.v. with 2 μg α-GalCer ($n = 14$) at 16.5 dpc. After 2 h, mice were injected s.c. with rosiglitazone (10 mg/kg body weight; Selleck Chemicals, Houston, TX) diluted in 1:10 DMSO. Control pregnant mice received rosiglitazone only at 16.5 dpc ($n = 10$). Following injection, mice were monitored via video camera with infrared light until delivery (Fig. 2A).

Tissue collection from pregnant mice

Pregnant B6 mice were injected i.v. and/or s.c. at 16.5 dpc with DMSO, 2 μg α-GalCer, 2 μg α-GalCer followed 2 h later by rosiglitazone (10 mg/kg body weight), or rosiglitazone alone as a control. Mice were euthanized 6 h after the injection of α-GalCer or DMSO or 4 h after treatment with rosiglitazone ($n = 6$–10 mice/group). Decidual and myometrial tissues from one implantation site were collected, as previously described (82), and placed in RNAlater Stabilization Solution (Life Technologies, Grand Island, NY), according to the manufacturer's instructions. Decidual and myometrial tissues from the remaining implantation sites were collected, and leukocytes were immediately isolated. The spleen, uterine lymph nodes (ULNs), and liver were also collected, and leukocyte suspensions were prepared.

Leukocyte isolation from murine tissues

Isolation of leukocytes from myometrial and decidual tissues was performed as previously described (82). Briefly, tissues were cut into small pieces using fine scissors and enzymatically digested with StemPro Cell Dissociation Reagent (Accutase; Life Technologies) for 35 min at 37°C. The spleen, ULNs, and liver were gently dissociated using two glass slides to prepare a single leukocyte suspension. Leukocyte suspensions were filtered using a 100-μm cell strainer (Fisher Scientific, Hanover Park, IL) and washed with FACS buffer (0.1% BSA [Sigma-Aldrich] and 0.05%

sodium azide [Fisher Scientific Chemicals, Fair Lawn, NJ] in 1× PBS [Fisher Scientific Bioreagents]) before immunophenotyping.

Immunophenotyping of murine leukocytes

Leukocyte suspensions from decidual and myometrial tissues and the liver were stained using the LIVE/DEAD Fixable Blue Dead Cell Stain Kit (Life Technologies) prior to incubation with extracellular mAbs. Leukocyte suspensions were centrifuged, and cell pellets were incubated for 10 min with the CD16/CD32 mAb (FcγIII/II Receptor; BD Biosciences, San Jose, CA) and subsequently incubated with specific fluorochrome-conjugated anti-mouse mAbs (Supplemental Table I) for 30 min. Leukocyte suspensions were lysed/fixed with Lyse/Fix Buffer for extracellular staining and were fixed/permeabilized with the BD Cytofix/Cytoperm Fixation/Permeabilization Solution Kit (both from BD Biosciences) for intracellular staining. At least 50,000 events for the spleen, liver, and decidual cells or 25,000 events for the ULNs and myometrial cells were acquired using the BD LSRFortessa flow cytometer and FACSDiva 8.0 software (both from BD Biosciences). Leukocyte subsets were gated within the viability gate. Immunophenotyping included identification of CD1d-restricted iNKT cells (CD1d Tetramer$^+$DX5$^+$NK1.1$^+$TCRβ$^+$ cells) and their activation status by expression of CD69, CD44, IFN-γ, and IL-4; conventional T cells (CD3$^+$CD4$^+$ and CD3$^+$CD8$^+$ cells) and their activation status by expression of CD69, CD25, PD1, CD40L, and CTLA-4; neutrophils (CD11b$^+$Ly6G$^+$ cells) and their activation status by expression of IFN-γ; and macrophages (CD11b$^+$F4/80$^+$ cells) and their activation status by expression of Arg1, iNOS, IFN-γ, and IL-10; as well as the expression of IFN-γ by mature dendritic cells (DCs) (CD11b$^+$CD11c$^+$DEC205$^+$ cells). Data were analyzed using FACSDiva 8.0 software. The total number of specific leukocytes was determined using CountBright absolute counting beads (Molecular Probes, Eugene, OR). The figures were prepared using FlowJo software version 10 (TreeStar, Ashland, OR).

Gene expression determination

RNA was extracted from decidual and myometrial tissues using TRIzol reagent (Life Technologies), QIAshredders, RNase-Free DNase Sets, and RNeasy Mini Kits (all from QIAGEN, Valencia, CA). RNA concentrations and purity were assessed with the NanoDrop 1000 spectrophotometer (Thermo Scientific, Wilmington, DE), and RNA integrity was evaluated with the Bioanalyzer 2100 (Agilent Technologies, Wilmington, DE). cDNA was synthesized using RT^2 First Strand Kits (QIAGEN). The RT^2 Profiler Mouse PPAR Targets PCR Array and RT^2 Profiler Mouse Inflammatory Cytokines & Receptors PCR Array (both from QIAGEN) were used for initial screening (n = 4 samples/group) and performed using RT^2 SYBR Green ROX qPCR MasterMix (QIAGEN) on a 7500 Fast Real-Time PCR System (Applied Biosystems, Life Technologies, Foster City, CA). Expression profiling of those genes selected based on the screening results was confirmed by quantitative real-time PCR (qRT-PCR) using a BioMark high-throughput qRT-PCR System (Fluidigm, San Francisco, CA) and an ABI 7500 FAST Real-Time PCR System using TaqMan gene expression assays (both from Applied Biosystems) (n = 6–8 mice/group; Supplemental Table II).

Serum cytokine/chemokine concentrations

Pregnant B6 mice were injected at 16.5 dpc with DMSO, 2 μg α-GalCer, 2 μg α-GalCer followed 2 h later by rosiglitazone (10 mg/kg body weight), or rosiglitazone alone as a control. Mice were euthanized 6 or 24 h after the injection with α-GalCer or DMSO (n = 8–9 mice/group). Blood was recovered by cardiac puncture, and serum samples were separated by centrifugation and stored at −20°C until analysis. The Milliplex MAP Mouse Cytokine/Chemokine Kit (MCYTOMAG-70K-PX32; EMD Millipore, Billerica, MA) was used to measure the concentrations of G-CSF, GM-CSF, IFN-γ, IL-1α, IL-1β, IL-2, IL-3, IL-4, IL-5, IL-6, IL-7, IL-9, IL-10, IL-12p40, IL-12p70, IL-13, IL-15, IL-17, CCL11, CXCL10, CXCL1, LIF, CXCL5, CCL2, M-CSF, CXCL9, CCL3, CCL4, CXCL2, CCL5, and TNF-α in the serum samples, according to the manufacturer's instructions. Plates were read using the Luminex 100 System, and analyte concentrations were calculated using xPONENT 3.1 software (both from Luminex, Austin, TX). The sensitivities of the assays (all in pg/ml) were 1.7 (G-CSF), 1.9 (GM-CSF), 1.1 (IFN-γ), 10.3 (IL-1α), 5.4 (IL-1β), 1.0 (IL-2), 1.0 (IL-3), 0.4 (IL-4), 1.0 (IL-5), 1.1 (IL-6), 1.4 (IL-7), 17.3 (IL-9), 2.0 (IL-10), 3.9 (IL-12p40), 4.8 (IL-12p70), 7.8 (IL-13), 7.4 (IL-15), 0.5 (IL-17), 1.8 (CCL11), 0.8 (CXCL10), 2.3 (CXCL1), 1.0 (LIF), 22.1 (CXCL5), 6.7 (CCL2), 3.5 (M-CSF), 2.4 (CXCL9), 7.7 (CCL3), 11.9 (CCL4), 30.6 (CXCL2), 2.7 (CCL5), and 2.3 (TNF-α). Interassay and intra-assay coefficients of variation were <15% and <4.9%, respectively.

Human samples

Chorioamniotic membrane and basal plate samples were collected within 30 min after delivery from the Bank of Biological Specimens of the Perinatology Research Branch, an intramural program of the Eunice Kennedy Shriver National Institute of Child Health and Human Development, National Institutes of Health, U. S. Department of Health and Human Services, Wayne State University, and The Detroit Medical Center (Detroit, MI). The Institutional Review Boards approved the collection and use of biological materials for research purposes. All participating women provided written informed consent. The study groups included women who delivered at term without labor (TNL), at term with labor (TIL), preterm without labor (PTNL), and preterm with labor (PTL). Demographic and clinical characteristics of these study groups are shown in Table I. Patients with multiple births or with neonates having congenital or chromosomal abnormalities were excluded. Labor was defined by the presence of regular uterine contractions at a frequency of at least two

Table I. Demographic and clinical characteristics of the study populations

Demographic or Clinical Characteristic	TNL (n = 7)	TIL (n = 26)	PTNL (n = 13)	PTL (n = 14)	p Value
Maternal age (y; median [interquantile range])[a]	28 (23–32)	23.5 (22–27)	25 (22–30)	22 (19.5–25)	NS
Race (n [%])[b]					NS
African-American	7 (100)	26 (100)	11 (84.6)	13 (92.9)	
White	0 (0.0)	0 (0.0)	1 (7.7)	1 (7.1)	
Hispanic	0 (0.0)	0 (0.0)	0 (0.0)	0 (0.0)	
Other	0 (0.0)	0 (0.0)	1 (7.7)	0 (0.0)	
Maternal weight (kg; median [interquantile range])[a]	93 (68.8–98.7)	90.05 (71.1–106.0)	74.8 (62.6–102.7)	75.6 (56.7–88.2)	NS
Body mass index (kg/m^2; median [interquantile range])[a]	31.2 (26.35–41.45)	33.9 (27.38–39.25)	32.8 (23–39.4)	28.35 (21.53–31.6)	NS
Primiparity (n [%])[b]	0 (0)	6 (23.08)	3 (23.08)	1 (7.14)	NS
Gestational age at delivery (wk; median [interquantile range])[a]	39 (38.5–39.5)	39.4 (38.2–39.9)	34.9 (32–36.1)	34.2 (31.2–35.3)	<0.0001
Birth weight (g; median [interquantile range])[a]	3005 (2855–3073)	3240 (2906–3419)	1510 (1255–2375)	2148 (1674–2554)	<0.0001
Cesarean section (%)[b]	100	15.4	100	14.3	<0.0001
Chronic chorioamnionitis (%)[b]	28.6	30.8	46.2	21.4	NS
Acute chorioamnionitis (%)[b]	0	34.6	7.7	42.8	NS
Smoked during pregnancy (n [%])[b]					NS
Yes	1 (14.3)	5 (19.2)	2 (15.4)	0 (0)	
No	6 (85.7)	21 (80.8)	11 (84.6)	14 (100)	

[a]Kruskal–Wallis test.
[b]χ^2 test.

contractions every 10 min, with cervical changes resulting in delivery (83). In each case, several tissue sections of the chorioamniotic membranes, umbilical cord, and placental disc were evaluated for acute chorioamnionitis and chronic chorioamnionitis, according to published criteria (84, 85), by pathologists who had been blinded to the clinical outcome.

Decidual leukocyte isolation from human samples

Decidual leukocytes from human decidual tissue were isolated as previously described (86). Briefly, the decidua basalis was collected from the basal plate of the placenta, and the decidua parietalis was separated from the chorioamniotic membranes (Fig. 8A). Decidual tissue was homogenized using a gentleMACS Dissociator (Miltenyi Biotec, San Diego, CA) in StemPro Cell Dissociation Reagent. Homogenized tissues were incubated for 45 min at 37˚C with gentle agitation. After incubation, tissues were washed with ice-cold 1× PBS (Life Technologies) and filtered through a 100-μm cell strainer. Cell suspensions were collected and centrifuged at 300 × *g* for 10 min, and the cell pellet was suspended in FACS buffer. Mononuclear leukocytes were purified using a density gradient (Ficoll-Paque Plus; GE Healthcare Bio-Sciences, Uppsala, Sweden), following the manufacturer's instructions. Lastly, mononuclear cell suspensions were washed using FACS buffer before immunophenotyping.

Immunophenotyping of human decidual leukocytes

Mononuclear cell suspensions from decidual tissues were stained with BD Horizon Fixable Viability Stain 510 dye (BD Biosciences) prior to incubation with extracellular mAbs. Mononuclear cell suspensions were washed with staining buffer (cat. no. 554656; BD Biosciences) and centrifuged. Cell pellets were incubated for 10 min with FcR Blocking Reagent (cat. no. 130-059-901; Miltenyi Biotec). Next, mononuclear cell suspensions were incubated with the following fluorochrome-conjugated anti-human mAbs: CD14-BUV395 (clone MΦP9), CD15-BV605 (clone W6D3), CD3-BV650 (clone OKT3), CD19-BUV737 (clone SJ25C1), CD56–PE-Cy7 (clone NCAM16.2), CD69–Alexa Fluor 700 (clone FN50; all from BD Biosciences), and Vα24Jα18TCR-PE (clone 6B11; eBioscience, San Diego, CA) for 30 min at 4˚C in the dark. Finally, mononuclear cell suspensions were washed and resuspended in 0.5 ml staining buffer and acquired using the BD LSRFortessa flow cytometer and FACSDiva 6.0 software. Leukocyte subsets were gated within the viability gate, and activated iNKT-like cells were identified as $CD15^{-}CD14^{-}CD19^{-}CD3^{+}CD56^{+}CD69^{+}$ or $CD3^{+}Vα24Jα18TCR^{+}CD69^{+}$ cells. The analysis was performed, and the figures were generated using FlowJo software version 10.

Immunofluorescence

Immediately after collection, the chorioamniotic membranes were frozen in Tissue-Plus O.C.T. Compound (Fisher HealthCare, Houston, TX). Ten-micron-thick cryosections were cut, placed on Fisherbrand Superfrost Plus microscope slides (Thermo Scientific, Waltham, MA), fixed with 4% paraformaldehyde (Electron Microscopy Sciences, Hatfield, PA), and washed with 1× PBS. Nonspecific Ab interaction was blocked using a Protein Blocker serum-free (cat. no. X0909; Dako North America, Carpinteria, CA) for 30 min at room temperature. Slides were incubated with the following anti-human mAbs: mouse CD69-FITC (LifeSpan BioSciences, Seattle, WA), mouse CD56-allophycocyanin (clone MEM-188; BioLegend, San Diego, CA), and rabbit CD3 (Abcam, Cambridge, MA) at 4˚C overnight. Following incubation, slides were washed with 1× PBS containing 0.1% Tween-20 (Sigma-Aldrich). Secondary goat anti-rabbit IgG–Alexa Fluor 594 (Invitrogen, Molecular Probes) was added for CD3 detection, and slides were incubated for 1 h at room temperature. Slides were washed and mounted with ProLong Gold Antifade reagent with DAPI (Life Technologies). Immunofluorescence was visualized using a Zeiss LSM 780 laser scanning confocal microscope (Carl Zeiss Microscopy, Jena, Germany) at the Microscopy, Imaging, and Cytometry Resources Core at Wayne State University School of Medicine (http://micr.med.wayne.edu/). Immunofluorescence signals for allophycocyanin, Alexa Fluor 594, and FITC were excited using a 633-nm HeNe laser, a 561-nm HeNe laser, and the 488-nm line of a Multiline Argon laser, respectively. The DAPI signal was excited using a 405-nm diode laser.

Statistical analysis

Observational mouse data were analyzed using IBM SPSS, version 19.0, and all other analyses were performed in R (http://www.R-project.org/). For the gestational age, rate of pup mortality, and ultrasound parameters, the statistical significance of group comparisons was assessed using Mann–Whitney *U* tests. For flow cytometry data, the statistical significance of group comparisons was assessed using Mann–Whitney *U* tests. For fetal, placental, and neonatal weights, the statistical significance of group comparisons was assessed using pooled variance *t* tests after log transformation. For qRT-PCR arrays, negative ΔCt values were determined using multiple reference genes (*Gusb*, *Hsp90ab1*, *Gapdh*, and *Actb*) averaged within each sample to determine gene expression levels. A heat map was created for the group mean expression matrix (gene × group mean), with each gene expression level being standardized first. A hierarchical clustering tree of genes was constructed using 1-Pearson correlation as distance metric and average linkage, whereas treatment groups clustering was based on a euclidean distance with Ward linkage. For Fluidigm quantitative PCR assays, negative ΔCt values were calculated using *Actb* as a reference gene. For Fluidigm gene expression and cytokine concentrations, statistical tests of group differences were performed using linear models; if data were left-, right-, or interval-censored, a survival regression model with Gaussian error was used instead. Human demographic data were analyzed using IBM SPSS, version 19, and comparisons among the groups were performed using χ^2 tests for proportions, as well as Kruskal–Wallis tests for nonnormally distributed continuous variables. For proportions of activated iNKT-like cells in human decidual tissues, statistical significance of group differences was assessed using Mann–Whitney *U* tests. A p value < 0.05 was used to determine statistical significance.

Results

α-GalCer administration in the third trimester induces late PTB

Intravenous administration of 2 μg of α-GalCer during the third trimester caused 75 ± 18.9% of births to be categorized as late preterm (birth occurring between 18.0 and 18.5 dpc; α-GalCer–induced late PTB), whereas DMSO (control) resulted in no late PTBs (Fig. 1A). Consequently, dams that were injected i.v. with 2 μg of α-GalCer had shorter gestations than the DMSO control group (Fig. 1B). A high proportion of preterm pups was found dead minutes after delivery (Fig. 1C). Intravenous administration of 3 or 4 μg of α-GalCer induced very early PTB (birth occurring before 17.5 dpc with 100% pup mortality); however, 1 μg of α-GalCer did not cause PTB (data not shown). These data demonstrate that α-GalCer administration in the third trimester induces late PTB and pup mortality.

α-GalCer administration in the third trimester causes neonatal death

Dams that were injected with α-GalCer delivered premature viable and nonviable pups. We then investigated whether these pups were dying in the uterus (fetal death) or after delivery (neonatal death). Abnormal umbilical artery velocimetry and fetal heart rate are associated with fetal compromise (87–90). Therefore, Doppler ultrasound was performed on 17.5 dpc, just prior to late PTB in those mice injected with α-GalCer. The umbilical artery pulsatility index did not differ between fetuses from dams injected with α-GalCer and DMSO (Fig. 1D). However, bradycardia, a reduction in the heart rate, occurred in fetuses from dams injected with α-GalCer (Fig. 1E). These data demonstrated that, although pups did not die in the uterus, their health was compromised before birth. Administration of α-GalCer also reduced fetal and placental weights but did not decrease the weight of 1-wk-old neonates (Supplemental Fig. 1). To further evaluate when the premature pups died, we placed dams injected with α-GalCer under video surveillance using infrared thermography. A high proportion of premature pups died within 10 min of delivery. In Fig. 1F, representative frames demonstrate that the body temperature of a nonviable premature pup (red circle) decreased quickly from 30.5 to 21.3˚C. Conversely, a viable premature pup kept a constant temperature of 23.1–23.3˚C (green circle).

α-GalCer administration in the second trimester does not cause pregnancy loss

During midpregnancy, iNKT cell activation by i.p. administration of α-GalCer (100 μg/kg of body weight, ∼2.5 μg) leads to pregnancy loss (91, 92). We demonstrated that i.v. administration

A

Injection/ Rate	Term Birth	Late Preterm Birth	Fisher's Exact Test
DMSO	100% (19/19)	0% (0/19)	p<0.0001
α-GalCer	25±9.5% (5/20)	75±18.9% (15/19)	

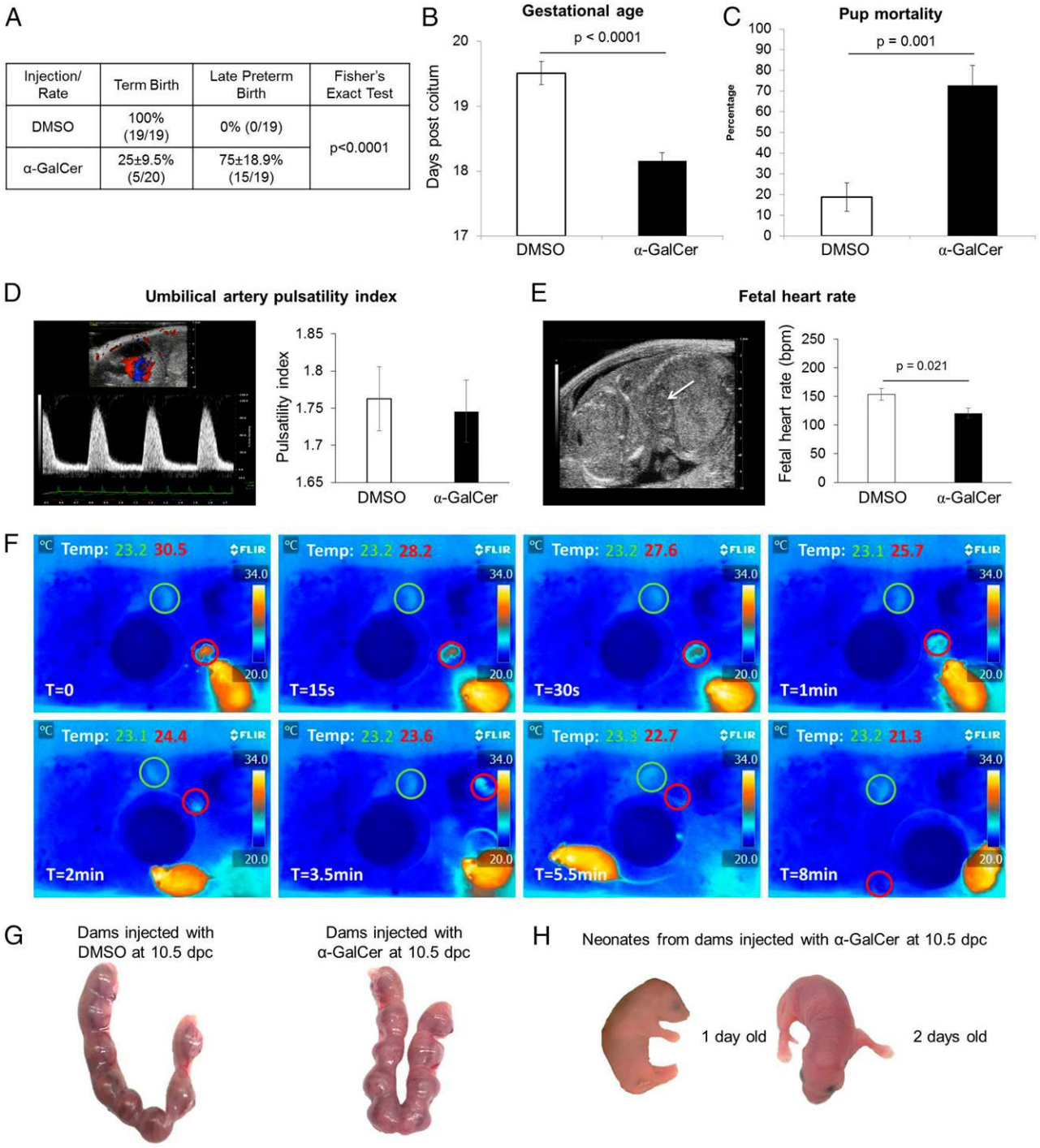

FIGURE 1. α-GalCer induces late PTB but not pregnancy loss. (**A**) The rate of term birth was defined as the percentage of dams delivering at 19.5 ± 0.5 dpc among all births. The rate of late PTB was defined as the percentage of dams delivering between 18.0 and 18.5 dpc among all births. Data are shown as percentage ± 95% confidence interval. (**B**) Gestational age was calculated from the presence of the vaginal plug (0.5 dpc) until the observation of the first pup in the cage bedding. (**C**) The rate of pup mortality for each litter was defined as the proportion of born pups found dead among the total litter size. Data in (A–C) are from individual dams (n = 19–20 each). (**D** and **E**) Doppler ultrasound was performed on fetuses just prior to α-GalCer–induced late PTB in dams injected with α-GalCer and in time-matched DMSO controls. Umbilical artery pulsatility index and fetal heart rate were recorded. Data are from three independent litters. (**F**) Immediately after α-GalCer–induced late PTB, the body temperature of the newborns was monitored using a thermal infrared camera. Temperature readings were recorded at 0, 15, and 30 s, as well as at 1, 2, 3.5, 5.5, and 8 min. Data are representative of individual dams (n = 3). (**G**) Uterine horns at 14.5 dpc from dams injected i.v. with DMSO or α-GalCer on 10.5 dpc. Data are representative of individual dams (n = 5 each). (**H**) Term neonates at 1 and 2 d old delivered from dams injected i.v. with α-GalCer on 10.5 dpc. Data are representative of individual dams (n = 3).

of 2 μg of α-GalCer in the second trimester did not cause pregnancy loss (Fig. 1G). However, we could not rule out the possibility that this dose would cause PTB or have deleterious effects on neonates. Therefore, neonates from dams injected with α-GalCer at 10.5 dpc were observed up to 1 wk postpartum. All delivered pups were viable and appeared healthy. Fig. 1H shows viable term pups at 1 and 2 d postpartum from dams injected with α-GalCer in the second trimester.

Rosiglitazone treatment reduces the rate of α-GalCer–induced late PTB

iNKT cell activation can initiate the NF-κB pathway, leading to production of Th1 cytokines, such as IFN-γ (67). We then hypothesized that activation of the PPARγ pathway by administration of rosiglitazone, which interferes with the NF-κB pathway (75, 76), would prevent α-GalCer–induced late PTB. Dams that were injected with α-GalCer and subsequently treated with rosiglitazone had a 40% reduction in the rate of late PTB in comparison with dams injected with α-GalCer alone (35.7 ± 25.1% versus 75 ± 18.9%, Fig. 2B). Consequently, gestational age was greater in dams treated with rosiglitazone after α-GalCer injection than in dams injected with α-GalCer alone (Fig. 2C). Importantly, dams treated with rosiglitazone after an injection of α-GalCer had a 30% reduction in pup mortality compared to dams injected with α-GalCer alone (Fig. 2D). These results demonstrate that treatment with rosiglitazone can prevent α-GalCer–induced late PTB and improve neonatal outcomes.

α-GalCer inhibits PPARγ activation at the maternal–fetal interface that is restored by rosiglitazone

Because treatment with rosiglitazone reduced the rate of α-GalCer–induced late PTB, we investigated whether α-GalCer was inhibiting PPARγ genes at the maternal–fetal interface and whether this inhibition could be abrogated by rosiglitazone. Expression profiles of the PPAR pathway–related genes were different between myometrial and decidual tissues in all of the groups (Fig. 2E). We specifically focused on PPARγ target genes. Adipocyte-specific fatty acid binding protein 4 (Fabp4) and fatty acid transport protein 4 (Fatp4) are recognized as indicators of PPARγ activation (93, 94). Our array data showed that rosiglitazone upregulated *Fabp4* in myometrial tissues and *Fatp4* and *Cyp410* in decidual tissues, whereas α-GalCer downregulated such genes; therefore, we validated the expression of *Fabp4* and *Fatp4* in these tissues. Administration of α-GalCer downregulated expression of *Fabp4* in myometrial tissues; however, treatment with rosiglitazone resulted in upregulation to basal levels (Fig. 2F). Administration of α-GalCer downregulated

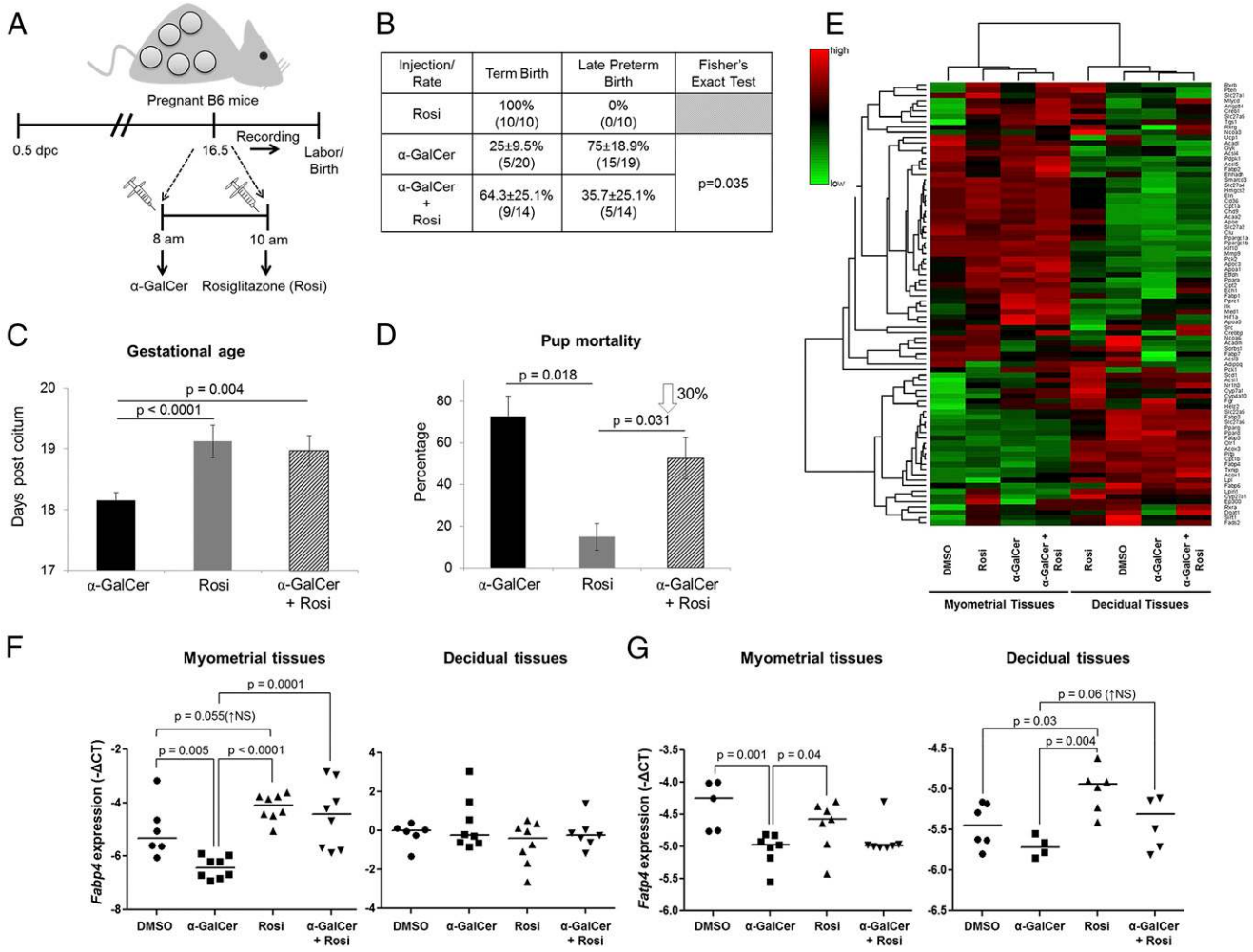

FIGURE 2. Rosiglitazone treatment reduces the rate of α-GalCer–induced late PTB by inducing PPARγ activation at the maternal–fetal interface. (**A**) On 16.5 dpc, pregnant mice were injected i.v. with α-GalCer and treated shortly after with rosiglitazone (Rosi; s.c.) and monitored via video camera (n = 14). Control mice were injected s.c. with rosiglitazone alone (n = 10). (**B**) The rate of term birth was defined as the percentage of dams delivering at 19.5 ± 0.5 dpc among all births. The rate of late PTB was defined as the percentage of dams delivering between 18.0 and 18.5 dpc among all births. Data are represented as percentage ± 95% confidence interval. (**C**) Gestational age was calculated from the presence of the vaginal plug (0.5 dpc) until the observation of the first pup in the cage bedding. (**D**) The rate of pup mortality for each litter was defined as the proportion of born pups found dead among the total litter size. (**E**) A heat map visualization of PPAR targets gene expression in myometrial and decidual tissues from dams injected with DMSO, α-GalCer, Rosi, or α-GalCer + Rosi. Data are from individual dams (n = 4 each). mRNA expression of *Fabp4* (**F**) and *Fatp4* (**G**) in myometrial and decidual tissues. Negative ΔCT values (F and G) were calculated using *Actb* as a reference gene. Data are from individual dams (n = 6–8 each).

expression of *Fatp4* in myometrial tissues and tended to downregulate expression of *Fatp4* in decidual tissues (Fig. 2G). Treatment with rosiglitazone partially restored *Fatp4* expression in decidual tissues but not in myometrial tissues (Fig. 2G). These results demonstrate that rosiglitazone prevents α-GalCer–induced late PTB by restoring PPARγ activation at the maternal–fetal interface.

α-GalCer induces an expansion of activated CD1d-restricted iNKT cells in decidual tissues that is blunted by rosiglitazone

Next, we investigated whether α-GalCer caused a systemic and local (maternal–fetal interface) expansion of iNKT cells and whether rosiglitazone reduced such expansions. Because NKT cell function and subsets are tissue or organ specific (95–97), we used a combination of markers, including CD1d-Tetramer loaded with α-GalCer, DX5, NK1.1, and TCRβ to identify iNKT cells (Fig. 3A). Administration of α-GalCer caused an expansion of CD1d-restricted iNKT cells (CD1d Tetramer$^+$DX5$^+$TCRβ$^+$NK1.1$^+$ cells) in decidual tissues, yet this expansion was blunted by treatment with rosiglitazone (Fig. 3B). In contrast, administration of α-GalCer did not significantly alter the number of CD1d-restricted iNKT cells in the liver (Supplemental Fig. 2A), myometrium (Supplemental Fig. 2B), spleen (Supplemental Fig. 2C), or ULNs (Supplemental Fig. 2D).

We also evaluated whether α-GalCer–expanded decidual iNKT cells were activated and, in such a case, whether rosiglitazone treatment reduced the number of these cells. Activated iNKT cells express CD69 and CD44 and release Th1 (e.g., IFN-γ) and Th2 (e.g., IL-4) cytokines (67, 69, 98). Decidual CD1d-restricted iNKT cells expressed CD69, CD44, IL-4 (Fig. 3C), and, to a lesser extent, IFN-γ (Supplemental Fig. 3). Administration of α-GalCer increased the number of activated CD69$^+$CD44$^+$ and IL-4$^+$CD1d-restricted iNKT cells in decidual tissues, both of which were reduced by treatment with rosiglitazone (Fig. 3D, 3E). No significant effects were seen in IFN-γ$^+$CD1d-restricted iNKT cells upon α-GalCer and/or rosiglitazone administration (Supplemental Fig. 3). Together, these data demonstrate that rosiglitazone prevents

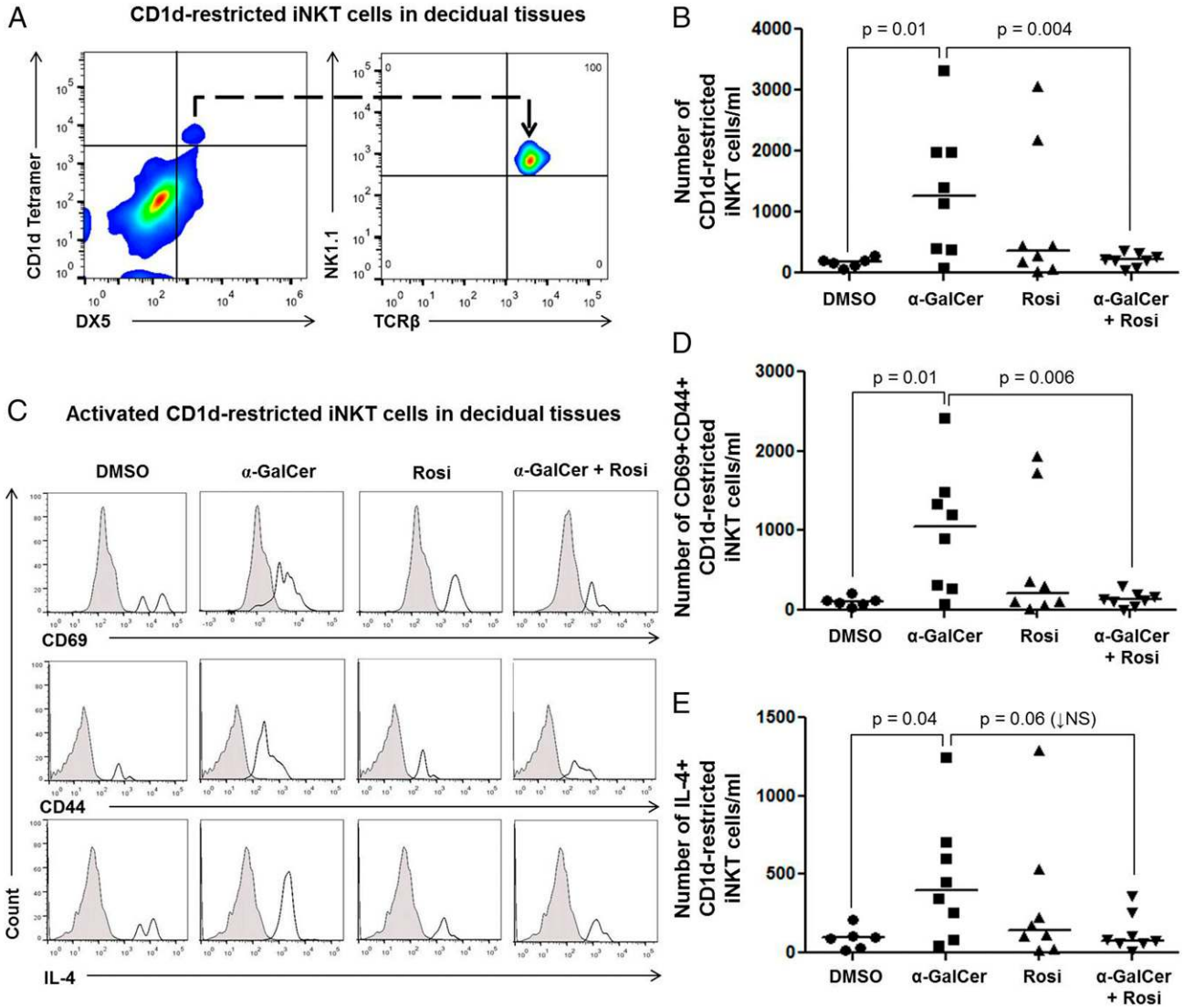

FIGURE 3. Administration of α-GalCer induces an expansion of activated CD1d-restricted iNKT cells in decidual tissues that is blunted by rosiglitazone. (**A**) Gating strategy used to identify CD1d-restricted iNKT cells (CD1d tetramer$^+$DX5$^+$NK1.1$^+$TCRβ$^+$ cells) in decidual tissues. (**B**) Number of CD1d-restricted iNKT cells in decidual tissues from mice injected with DMSO, α-GalCer, rosiglitazone (Rosi), or α-GalCer + Rosi. Data are from individual dams (n = 6–8 each). (**C**) Immunophenotyping of activation markers CD69, CD44, and IL-4 in CD1d-restricted iNKT cells in decidual tissues from mice injected with DMSO, α-GalCer, Rosi, or α-GalCer + Rosi. The shaded graph represents the autofluorescence control, and the open graph represents the fluorescence signal from CD1d-restricted iNKT cells. (**D** and **E**) Number of CD69$^+$CD44$^+$ and IL-4$^+$ CD1d-restricted iNKT cells in decidual tissues from mice injected with DMSO, α-GalCer, Rosi, or α-GalCer + Rosi. Data are from individual dams (n = 6–8 each).

α-GalCer–induced late PTB by reducing activated CD1d-restricted iNKT cells at the maternal–fetal interface.

α-GalCer induces activation of conventional CD4$^+$ T cells in myometrial tissues that is reduced by rosiglitazone

iNKT cells bridge the innate and adaptive limbs of the immune system; therefore, activation of iNKT cells triggers both innate and adaptive immune responses (99). Indeed, activation of CD1d-restricted iNKT cells by administration of α-GalCer in nonpregnant mice induces expression of CD69, an early activation marker, in T cells and B cells (100–103). We then investigated whether administration of α-GalCer in the third trimester induced T cell activation in myometrial and decidual tissues and whether this activation was reduced after treatment with rosiglitazone. Several markers of T cell activation, including CD25, CD40L, PD1, CD69, and CTLA-4, were determined in conventional CD4$^+$ and CD8$^+$ T cells. Administration of α-GalCer led to the activation of conventional CD4$^+$ T cells demonstrated by the expression of CD25 and PD1 in myometrial tissues, which was reduced by treatment with rosiglitazone (Fig. 4A–C). This treatment also reduced basal CD8$^+$ T cell activation in myometrial tissues (Fig. 4D, 4E). No significant effects were seen in activated CD4$^+$ and CD8$^+$ T cells upon α-GalCer administration in decidual tissues (Supplemental Fig. 4). These data demonstrate that rosiglitazone prevents α-GalCer–induced late PTB by reducing activated T cells in myometrial tissues.

α-GalCer induces innate immune activation at the maternal–fetal interface that is attenuated by rosiglitazone

iNKT cell activation also initiates innate immune responses mediated by macrophages and neutrophils (102, 104), as well as induces the full maturation of DCs manifested by the expression of MHC class II, IFN-γ production, and APC function (105).

First, we investigated whether administration of α-GalCer induces macrophage activation in myometrial and decidual tissues and whether this activation was reduced after treatment with rosiglitazone. Macrophage activation is a complex process because it depends on the nature of the stimulus and the microenvironment where these cells exhibit their function (106, 107). The classical M1/M2 macrophage paradigm provides useful markers (Arg1, iNOS, IL-10, and IFN-γ) for macrophage activation (108–111); therefore, we evaluated the expression of these molecules in myometrial and decidual macrophages (CD11b$^+$F4/80$^+$ cells). Administration of α-GalCer increased the number of decidual macrophages that produce both IFN-γ and IL-10 (Fig. 5A). Also, administration of α-GalCer increased the number of decidual macrophages that express both Arg1 and IL-10, yet this increase did not reach statistical significance (Fig. 5B). In both cases, treatment with rosiglitazone reduced the number of activated macrophages (Fig. 5A, 5B). Administration of α-GalCer did not have such effects on myometrial macrophages (data not shown).

Next, we investigated whether administration of α-GalCer induces neutrophil activation in myometrial and decidual tissues, and whether this activation was reduced after treatment with rosiglitazone. IFN-γ expression is an indicator of neutrophil activation (112, 113). We demonstrated that administration of α-GalCer increased the expression of IFN-γ by neutrophils in myometrial and decidual tissues, and this effect was reduced by treatment with rosiglitazone (Fig. 5C, Supplemental Fig. 5).

Lastly, we investigated whether administration of α-GalCer in the third trimester induced DC maturation in decidual tissues and whether this process was blocked by administration of rosiglitazone. Administration of α-GalCer increased the number of mature DCs (CD11b$^+$CD11c$^+$DEC205$^+$ cells; data not shown) and the number of IFN-γ$^+$ mature DCs in decidual tissues (Fig. 5D). Treatment with rosiglitazone did not reduce the number of mature DCs (data not shown); however, it reduced the number of IFN-γ$^+$ mature DCs in decidual tissues (Fig. 5D).

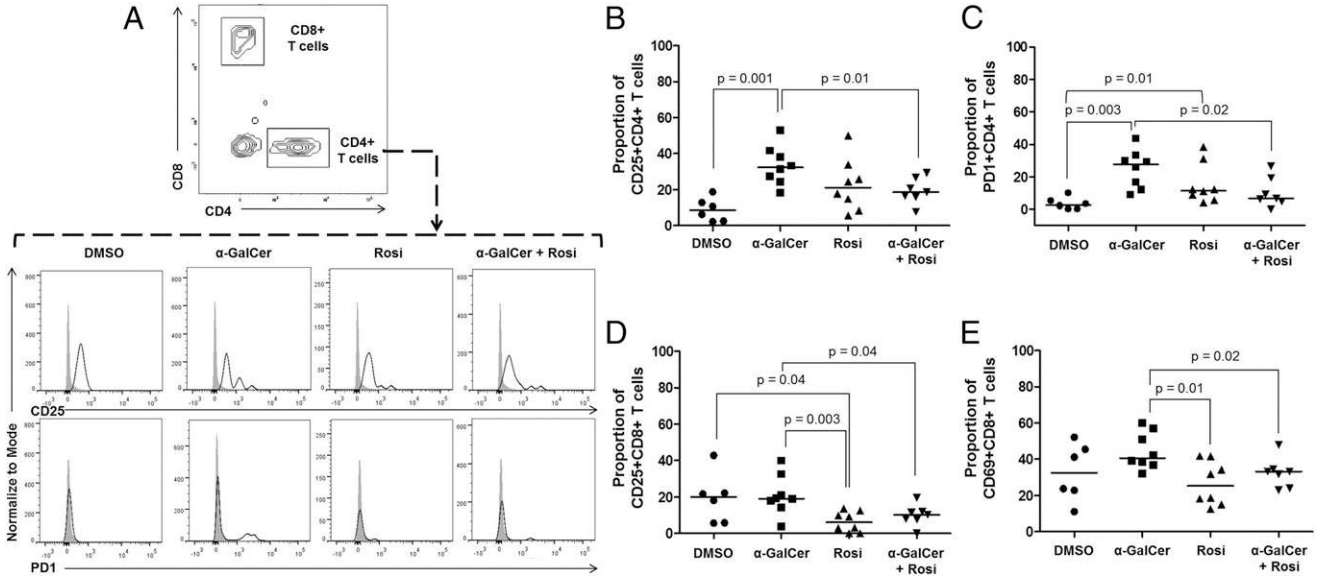

FIGURE 4. Administration of α-GalCer induces activation of CD4$^+$ T cells in myometrial tissues that is reduced by rosiglitazone. (**A**) Gating strategy used to identify activated CD4$^+$ T cells (CD3$^+$CD4$^+$ cells) in myometrial tissues. Immunophenotyping of activation markers CD25 and PD1 in CD4$^+$ T cells in myometrial tissues from mice injected with DMSO, α-GalCer, rosiglitazone (Rosi), or α-GalCer + Rosi. The shaded graphs represent the autofluorescence control, and the open graph represents the fluorescence signal from CD4$^+$ T cells. (**B** and **C**) Proportion of CD25$^+$CD4$^+$ T cells and PD1$^+$CD4$^+$ T cells in myometrial tissues from mice injected with DMSO, α-GalCer, Rosi, or α-GalCer + Rosi. Data are from individual dams (n = 6–8 each). (**D** and **E**) Proportion of CD25$^+$CD8$^+$ T cells and CD69$^+$CD8$^+$ T cells in myometrial tissues from mice injected with DMSO, α-GalCer, Rosi, or α-GalCer + Rosi. Data are from individual dams (n = 6–8 each).

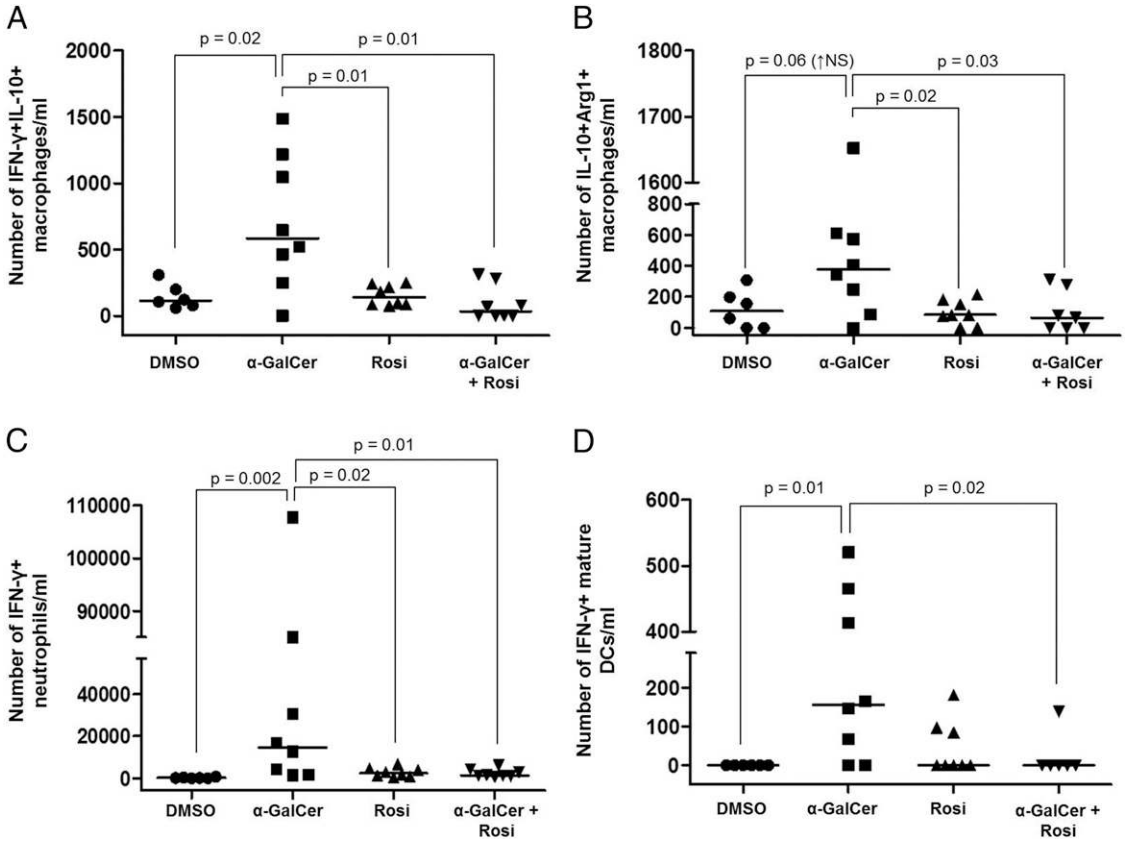

FIGURE 5. Administration of α-GalCer induces activation of innate immune cells at the maternal–fetal interface that is blunted by rosiglitazone. (**A**) Number of activated IFN-γ^+IL-10^+ macrophages in decidual tissues from mice injected with DMSO, α-GalCer, rosiglitazone (Rosi), or α-GalCer + Rosi. Data are from individual dams (n = 6–8 each). (**B**) Number of activated IL-10^+Arg1^+ macrophages in decidual tissues from mice injected with DMSO, α-GalCer, Rosi, or α-GalCer + Rosi. Data are from individual dams (n = 6–8 each). (**C**) Number of activated IFN-γ^+ neutrophils in decidual tissues from mice injected with DMSO, α-GalCer, Rosi, or α-GalCer + Rosi. Data are from individual dams (n = 6–8 each). (**D**) Number of IFN-γ^+ mature DCs in decidual tissue from mice injected with DMSO, α-GalCer, Rosi, or α-GalCer + Rosi. Data are from individual dams (n = 6–8 each).

Taken together, these data demonstrate that rosiglitazone prevents α-GalCer–induced late PTB by attenuating innate immune activation at the maternal–fetal interface.

α-GalCer induces a proinflammatory microenvironment at the maternal–fetal interface that is partially attenuated by rosiglitazone

Although iNKT cell activation induces the expression of inflammatory genes (65, 66), PPARγ activation suppresses their expression (75, 76). We next investigated whether α-GalCer upregulated inflammatory genes at the maternal–fetal interface and whether this upregulation was suppressed by rosiglitazone. Expression profiles of inflammation-related genes were different between decidual and myometrial tissues (Fig. 6A). As expected, several genes were upregulated in both types of tissue upon administration of α-GalCer (α-GalCer versus DMSO, Fig. 6A). Some of these genes were downregulated after treatment with rosiglitazone, mainly in decidual tissues (α-GalCer + Rosi versus α-GalCer, Fig. 6A). We selected some of the downregulated genes after treatment with rosiglitazone and validated their expression. Administration of α-GalCer upregulated the expression of *Ccl1*, *Ccl2*, *Ccl12*, and *Tnf* in decidual tissues; however, these genes were downregulated after treatment with rosiglitazone (Fig. 6B). Administration of α-GalCer also upregulated expression of *Ccl2* and *Ccl12* in myometrial tissues; however, only *Ccl2* was significantly downregulated after treatment with rosiglitazone (Fig. 6C). These data demonstrate that rosiglitazone prevents α-GalCer–induced late PTB by partially reducing the proinflammatory milieu at the maternal–fetal interface.

α-GalCer induces a maternal systemic proinflammatory response, yet rosiglitazone triggers a maternal systemic anti-inflammatory response

Next, we evaluated the effects of α-GalCer and rosiglitazone on maternal serum chemokine/cytokine concentrations at 6 or 24 h (prior to α-GalCer–induced late PTB) after α-GalCer administration. Six hours after α-GalCer administration, the concentrations of all measured cytokines, with the exception of GM-CSF, IL-3, IL-4, and IL-7, were increased compared to DMSO or rosiglitazone controls; however, none of these cytokines was reduced after treatment with rosiglitazone (data not shown). Twenty-four hours after α-GalCer administration, the proinflammatory cytokines IFN-γ, IL-2, CXCL9, CXCL10, CCL2, and CCL5 were increased compared to DMSO or rosiglitazone controls (Fig. 7A). Treatment with rosiglitazone did not reduce these high concentrations; indeed, it further increased the concentrations of IFN-γ, CXCL9, CXCL10, and CCL2 (Fig. 7A). Interestingly, dams injected with α-GalCer that were subsequently treated with rosiglitazone had increased concentrations of anti-inflammatory cytokines IL-10, IL-17, IL-3, IL-5, G-CSF, and IL-12p40 compared to mice injected with only α-GalCer (Fig. 7B). These data demonstrate that rosiglitazone prevents α-GalCer–induced late PTB by enhancing a maternal systemic anti-inflammatory response.

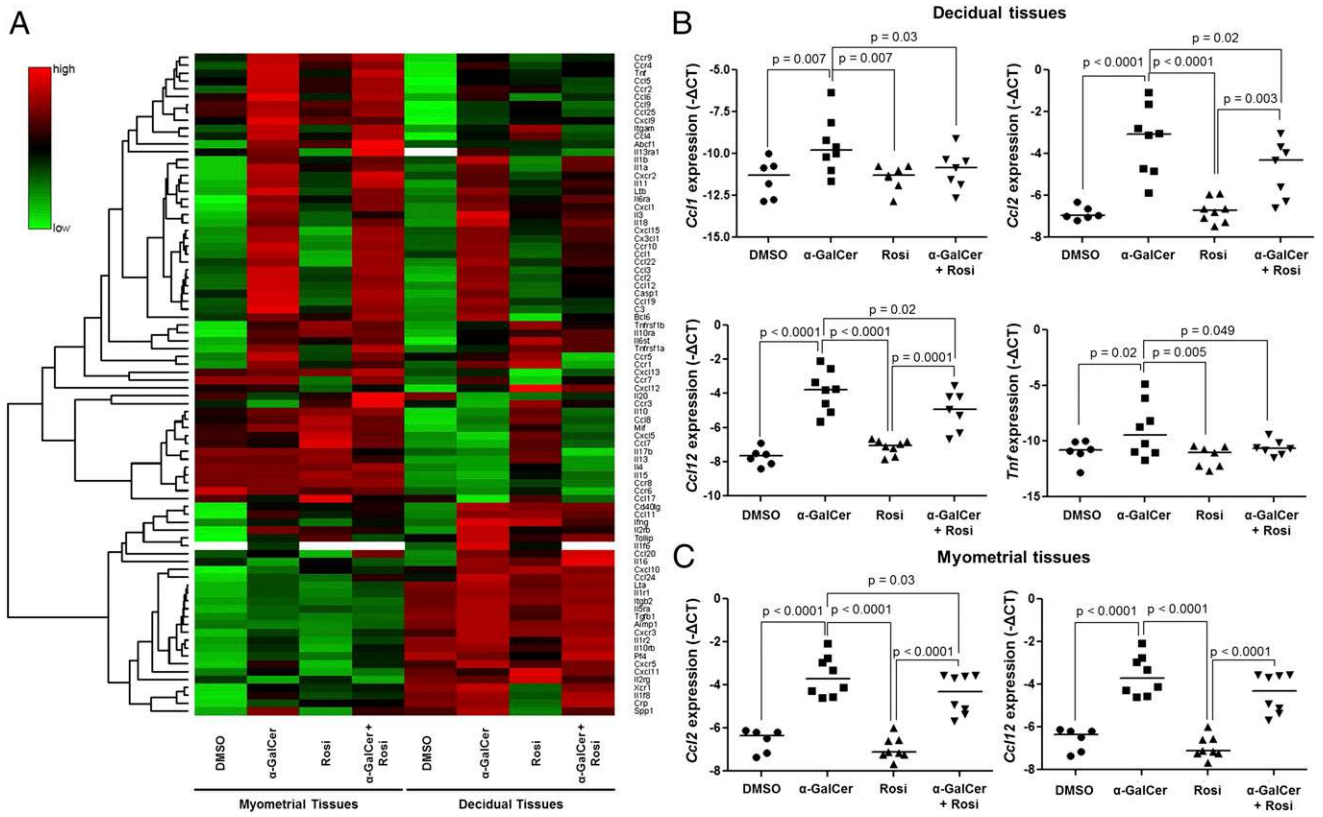

FIGURE 6. Administration of α-GalCer induces a proinflammatory microenvironment at the maternal–fetal interface that is partially attenuated by rosiglitazone. (**A**) A heat map visualization of cytokine and chemokine gene expression in myometrial and decidual tissues from dams injected with DMSO, α-GalCer, rosiglitazone (Rosi), or α-GalCer + Rosi. Data are from individual dams (n = 4 each). (**B**) mRNA expression of *Ccl1*, *Ccl2*, *Ccl12*, and *Tnf* in decidual tissues. Negative ΔCt values were calculated using *Actb* as a reference gene. Data are from individual dams (n = 6–8 each). (**C**) mRNA expression of *Ccl2* and *Ccl12* in myometrial tissues. Negative ΔCt values (B and C) were calculated using *Actb* as a reference gene. Data are from individual dams (n = 6–8 each).

Spontaneous preterm labor/birth is associated with an increased proportion of activated iNKT-like cells in decidual tissues

Up to this point, our results demonstrated that activation of decidual iNKT cells leads to late PTB in mice; however, it was unknown whether these cells are increased during preterm labor/birth in humans. iNKT cells are present in first-trimester decidua (114); therefore, we hypothesized that preterm labor will be associated with an increase in the proportion of activated iNKT cells at the maternal–fetal interface. In humans, the maternal–fetal interface includes the decidua parietalis, which lines the uterine cavity not covered by the placenta and is in juxtaposition to the chorion leave, and the decidua basalis, located in the basal plate of the placenta where it is invaded by interstitial trophoblasts (Fig. 8A). The gating strategy used to determine activated iNKT-like cells ($CD15^-CD14^-CD19^-CD3^+CD56^+CD69^+$ cells) in decidual tissues is shown in Fig. 8B. In the decidua basalis and decidua parietalis, activated iNKT-like cells were more abundant in women who underwent spontaneous term labor (TIL) or preterm labor (PTL) compared to women who did not undergo labor at term (TNL) or at preterm (PTNL), respectively (Fig. 8C, Table I). In the decidua basalis, activated iNKT-like cells were more abundant in PTL samples than in TIL samples (Fig. 8C). Further immunophenotyping of decidual samples (TIL and PTL, n = 4 each) revealed that activated iNKT cells ($CD3^+V\alpha24J\alpha18TCR^+CD69^+$ cells, Fig. 8D) were present at proportions similar to previously identified activated iNKT-like cells ($CD3^+CD56^+CD69^+$ cells) (Fig. 8B). Because we did not use the iNKT marker, Vα24Jα18TCR, in our initial immunophenotyping, we cannot refer to these as iNKT cells and have instead termed them iNKT-like cells. Localization of activated iNKT-like cells ($CD3^+CD56^+CD69^+DAPI^+$ cells, white arrows) in the decidua parietalis is shown in Fig. 8E. This last set of data demonstrates that activated iNKT-like cells in human decidual tissues are linked to spontaneous preterm labor/birth.

Discussion

Sterile intra-amniotic inflammation is more frequent than microbial-associated intra-amniotic inflammation in patients with spontaneous preterm labor (30, 57). Sterile inflammation is initiated by alarmins (55) and such danger signals are potent activators of iNKT cells (63, 64); therefore, we hypothesized that these innate lymphocytes participate in the pathophysiology of sterile inflammation-related preterm labor/birth. Using a high-affinity iNKT cell ligand, α-GalCer (73), we provide direct evidence that iNKT cell activation is implicated in the mechanisms that lead to inflammation-induced preterm labor in the absence of infection. Indirect evidence for the role of iNKT cells in the pathophysiology of inflammation-induced preterm labor was based on two facts: iNKT cell–null mice ($Ja18^{-/-}$ mice) are more resistant to endotoxin-induced PTB than wild-type mice (115), and adoptive transfer of decidual iNKT cells into iNKT cell–null mice injected with an endotoxin rapidly induces the onset of PTB (116). However, endotoxins are not iNKT cell ligands and can only activate autoreactive iNKT cells indirectly through TLR signaling and the release of IL-12 by APCs (68, 71, 117). Therefore, indirect activation of iNKT cells by an endotoxin resembles Gram-negative bacteria–related preterm labor, and direct

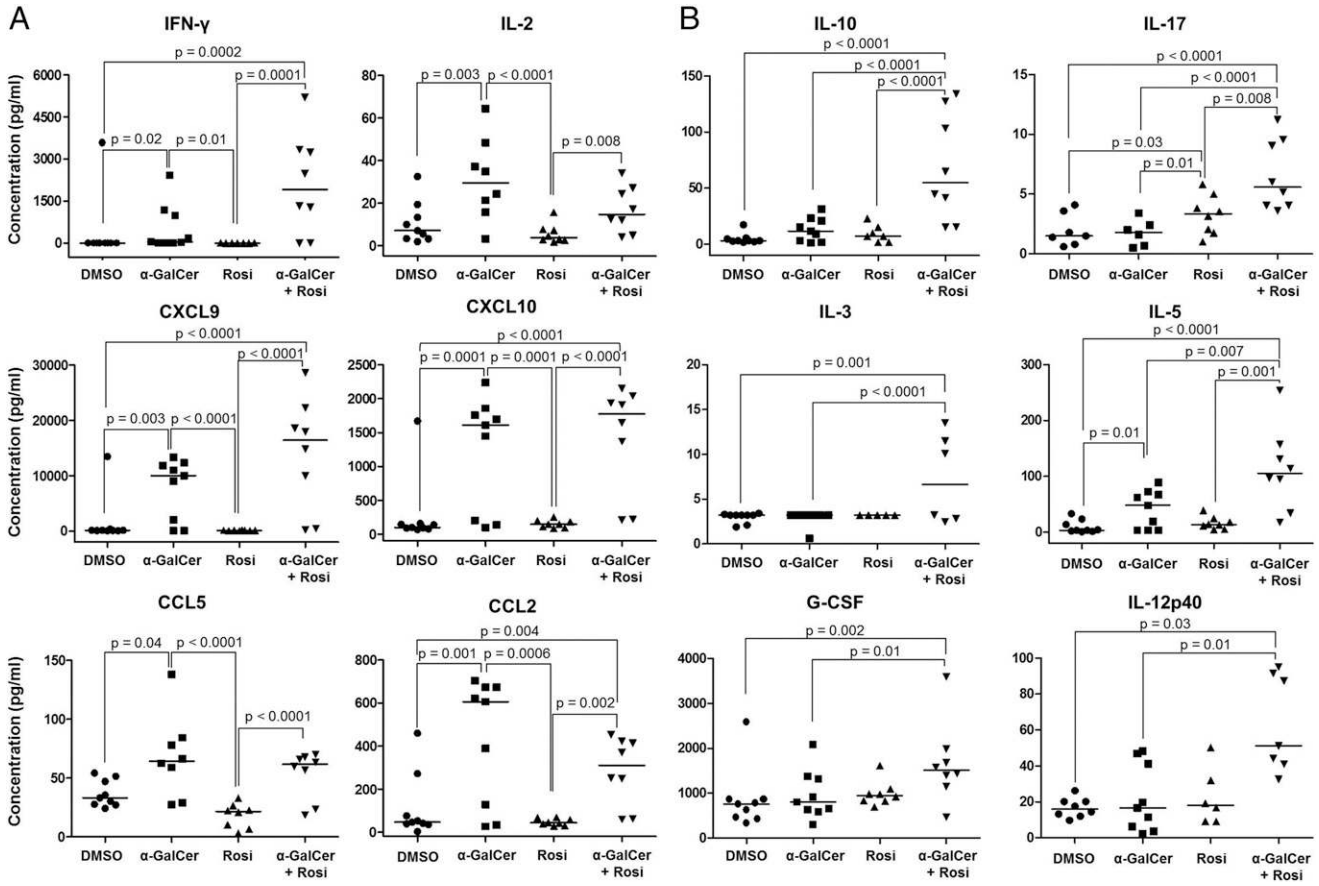

FIGURE 7. Administration of α-GalCer induces a maternal systemic proinflammatory response, yet rosiglitazone drives a maternal systemic anti-inflammatory response. Pregnant mice were injected with DMSO, α-GalCer, rosiglitazone (Rosi), or α-GalCer + Rosi. Serum concentrations of proinflammatory (**A**) and anti-inflammatory (**B**) cytokines/chemokines were determined 24 h after the initial injection. Data are from individual dams (n = 8–9 each).

activation via an iNKT cell ligand could explain sterile inflammation–related preterm labor.

Administration of α-GalCer in the second trimester did not result in pregnancy loss. This finding is not surprising because the mechanisms that lead to pregnancy loss differ from those implicated in preterm labor/birth. For example, during the second trimester, pregnancy maintenance depends on regulatory T cells (Tregs), because their depletion causes pregnancy loss (118, 119). However, in the third trimester, depletion of Tregs does not cause preterm labor/birth (120). These data led us to suggest that, during the third trimester, Treg-independent regulatory mechanisms, such as iNKT cell quiescence, may be responsible for pregnancy maintenance. Further studies are needed to investigate the mechanisms by which iNKT cells remain quiescent to maintain pregnancy until term.

Late preterm neonates survive, yet are at a higher risk for morbidity and mortality than term neonates (121, 122). In our model of α-GalCer–induced late PTB, we consistently showed that pups did not die in utero, yet they were bradycardic and died shortly after birth. This finding indicated that fetal compromise was occurring simultaneously with the process of preterm labor, rather than as a direct cause of prematurity. Because NKT cells appear at day 5 after birth (123), we are confident that the adverse neonatal outcomes are due to the effects of α-GalCer administration on the maternal immune system and at the maternal–fetal interface, rather than as a direct effect on the pups.

In this study, we demonstrated that α-GalCer inhibits PPARγ activation at the maternal–fetal interface, which is in line with a previous study demonstrating that PPARγ expression is reduced in intrauterine tissues in term parturition (124). These data suggest that PPARγ activation, a suppression of inflammatory genes, is required for late pregnancy maintenance, and its inhibition participates in the normal and pathological processes of labor. Conversely, rosiglitazone causes PPARγ activation and prevents α-GalCer–induced late PTB. Our observations, published in abstract form (125), demonstrated that this PPARγ agonist also prevents endotoxin-induced PTB. Therefore, targeting the PPARγ pathway could represent a new strategy to prevent both sterile and microbial inflammation–related preterm labor/birth.

An expansion of decidual iNKT cells was observed shortly after α-GalCer administration. This is consistent with a previous study demonstrating that iNKT cell activation is observed only 4 h after α-GalCer administration (92). A systemic expansion of iNKT cells occurs 2–3 d after α-GalCer administration (126), which explains why we did not observe such an event in our study. We also demonstrated that treatment with rosiglitazone attenuated the α-GalCer–induced iNKT cell expansion in decidual tissues. It is likely that rosiglitazone is interfering with iNKT cell development instead of causing cell death because this drug did not reduce viability in decidual cells (Supplemental Fig. 6), yet it caused a reduction of iNKT cells in the liver (Supplemental Fig. 2A). The previous hypothesis is supported by the fact that PPARγ activation regulates CD1d molecules (93, 127), which are constitutively expressed by APCs (128, 129) and can modulate iNKT cell responses (71, 130). Therefore, it is probable that indirect suppression of iNKT cell expansion and activation is the primary mechanism by

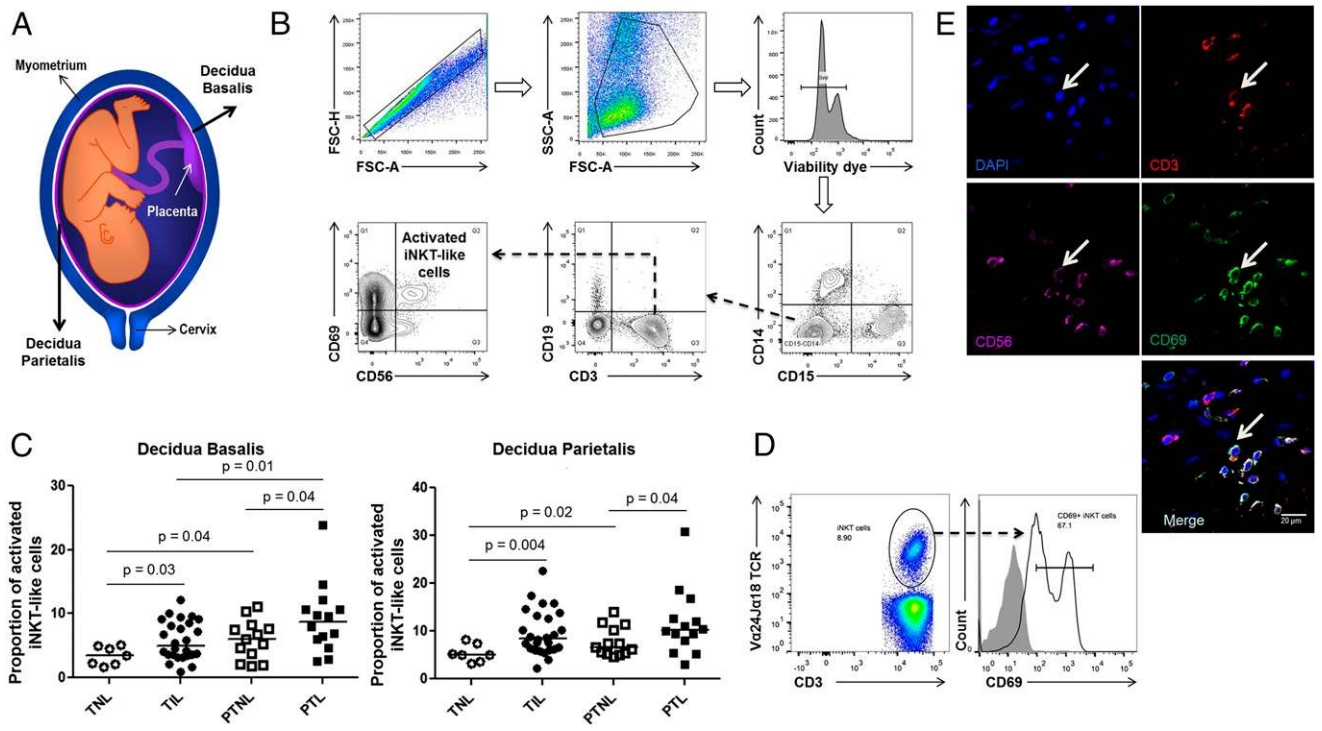

FIGURE 8. Spontaneous preterm labor/birth is associated with an increased proportion of activated iNKT-like cells in decidual tissues. (**A**) Schematic representation showing the decidua basalis and decidua parietalis. (**B**) Gating strategy used to identify activated iNKT-like cells ($CD69^+CD56^+CD3^+CD19^-CD14^-CD15^-$ cells) in human decidual tissue. (**C**) Activated iNKT-like cells in the decidual basalis or decidual parietalis from women who underwent spontaneous TIL or spontaneous PTL. Controls included samples from women who delivered at term (TNL) or preterm (PTNL) without labor. Data are from individual women: $n = 7$ for TNL, $n = 26$ for TIL, $n = 13$ for PTNL, and $n = 14$ for PTL. (**D**) Identification of $CD3^+V\alpha24J\alpha18TCR^+CD69^+$ cells in PTL decidual tissues. (**E**) Identification of activated iNKT-like cells in the decidua parietalis by confocal microscopy. Nuclei are blue (DAPI), $CD3^+$ cells are red (Alexa Fluor 594), $CD56^+$ cells are magenta (allophycocyanin), and $CD69^+$ cells are green (FITC). White arrows denote activated NKT cells. Scale bar, 20 μm.

which rosiglitazone prevents PTB in our model. Consequently, we investigated whether rosiglitazone could be suppressing activation/maturation of T cells, macrophages, neutrophils, and DCs, all of which are implicated in the pathophysiology of preterm labor/birth (47, 131, 132).

T cells seem to be implicated in the process of preterm parturition (132). This concept was based on the fact that mice deficient in T and B cells ($Rag1^{-/-}$) are more susceptible to endotoxin-induced PTB than wild-type mice, and this susceptibility is reversed upon transfer of $CD4^+$ T cells (133). These findings led us to suggest that $CD4^+$ T cells play a regulatory role in late pregnancy; however, their function has not been established by depleting these cells prior to preterm labor. Recently, we proposed that the activation of effector $CD4^+$ T cells is involved in the physiological process of parturition (134–136). In this study, we provide further evidence to support this hypothesis by demonstrating that activation of $CD4^+$ T cells occurs prior to α-GalCer–induced PTB. We also demonstrated that rosiglitazone reduced α−GalCer–induced T cell activation. This finding is consistent with previous studies demonstrating that pretreatment with PPARγ ligands reduces T cell activation and proliferation in vitro (137, 138). Taken together, these data support the hypothesis that $CD4^+$ T cell activation participates in the physiological and pathological processes of parturition and suggest that targeting the PPARγ pathway attenuates adaptive immune responses, rescuing preterm labor/birth.

The role of macrophages in the mechanisms that lead to preterm labor is well-established because depletion of these innate cells protects mice from endotoxin-induced PTB (139). In this study, we demonstrated increased macrophage activation prior to α-GalCer–induced PTB, which supports a central role for these innate immune cells in the proinflammatory milieu that accompanies the sterile processes of preterm parturition. We also found that treatment with rosiglitazone inhibits macrophage activation in decidual tissues. Prior research, in line with our study, showed that PPARγ expression is upregulated in activated macrophages and that treatment with rosiglitazone or natural PPARγ agonists downregulates the expression of iNOS, inhibits migration, and suppresses the release of inflammatory cytokines by these cells (75, 140, 141).

Unlike macrophages, the depletion of neutrophils does not prevent endotoxin-induced PTB, yet it ameliorates the proinflammatory response in the uterine–placental tissues (142). In this study, we demonstrated that activation of neutrophils occurs prior to α-GalCer–induced PTB, which suggests that, although neutrophils are not essential, they participate in the proinflammatory milieu that accompanies the pathological process of preterm parturition. Additionally, treatment with rosiglitazone reduced α-GalCer–induced neutrophil activation. This is in accord with a previous in vitro study that demonstrated that PPARγ agonists (troglitazone and 15-deoxy-$\Delta^{12,14}$ PG J_2) diminished the chemotactic response of neutrophils and suppressed their production of proinflammatory cytokines (143).

Administration of α-GalCer resulted in the expression of IFN-γ by mature decidual DCs. These innate immune cells seem to contribute to the initiation of T cell responses during the physiological and pathological processes of parturition (132, 133, 136, 144, 145). In this study, we provide evidence to support this hypothesis by demonstrating that mature DCs participate in the inflammatory process that leads to inflammation-related preterm labor/birth. We also showed that treatment with rosiglitazone blunted the

α-GalCer–induced IFN-γ expression in mature DCs but did not interfere with their maturation. This is in line with a previous study demonstrating that rosiglitazone does not interfere with the maturation of DCs in vitro or affect their ability to activate T cells in vivo; however, this PPARγ agonist modifies DC differentiation by reducing their secretion of cytokines (146).

Collectively, our results demonstrated that, prior to α-GalCer–induced PTB, there was an activation of innate immune cells at the maternal–fetal interface that was suppressed by rosiglitazone, rescuing inflammation-related preterm labor/birth.

In addition to regulating immune cell activation at the maternal–fetal interface, rosiglitazone attenuated the expression of proinflammatory cytokines/chemokines implicated in the pathophysiology of inflammation-related preterm labor (147–155). The suppressive effect of PPARγ agonists on cytokine expression was demonstrated previously in vitro (156). These data demonstrate that PPARγ activation regulates the local proinflammatory milieu associated with preterm labor/birth.

The systemic anti-inflammatory activity of rosiglitazone was also demonstrated in this study. This finding is concordant with our data showing that treatment with rosiglitazone increases the serum concentrations of IL-5 and CXCL9 in dams injected with an endotoxin (Y. Xu, R. Romero, D. Miller, L. Kadam, T.N. Mial, O. Plazyo, V. Garcia-Flores, S.S. Hassan, Z. Xu, A.L. Tarca, et al., unpublished observations). The immunomodulatory action of rosiglitazone, through the upregulation of anti-inflammatory cytokines, was demonstrated previously when PMA-stimulated THP-1 cells were incubated with PPARγ agonists, and an increased production of IL-1RA was observed (157). In our study, the anti-inflammatory effect of rosiglitazone was observed at 24 h, but not at 6 h, after α-GalCer administration, suggesting that the effect takes place after regulating the local microenvironment.

To conclude, we identified activated iNKT-like cells at the human maternal–fetal interface in term and preterm gestations. Activated iNKT-like cells were more abundant in the decidual basalis of women who underwent preterm labor than in those who delivered preterm without labor, suggesting that these cells are localized in a fetal antigenic site. The majority (92%) of our samples came from women who underwent spontaneous preterm labor and did not present intra-amniotic infection, which further supports the hypothesis that activated iNKT-like cells are implicated in the sterile process of inflammation that leads to preterm labor/birth.

In summary, this study demonstrates that in vivo iNKT cell activation leads to late preterm labor/birth by initiating innate and adaptive immune responses at the maternal–fetal interface. We also showed that iNKT cell activation exerts this effect by inducing a maternal systemic proinflammatory response. Finally, we demonstrated that PPARγ activation prevents prematurity by modulating the local and systemic inflammatory milieu that accompanies preterm labor. Further exploration of the PPARγ pathway and its regulation in pregnancy complications may lead to novel therapeutic approaches that can improve neonatal outcomes.

Acknowledgments

We thank Amy-Eunice Furcron, Elly N. Sanchez-Rodriguez, Derek Miller, Tara N. Mial, Mary Olive, Po Jen (Paul) Chiang, Amapola Balancio, Dr. Zhong Dong, and Lorri McLuckie for contributions to the execution of this study. We thank the physicians and nurses from the Center for Advanced Obstetrical Care and Research (Wayne State University) and the research assistants from the Perinatology Research Branch (Eunice Kennedy Shriver National Institute of Child Health and Human Development, National Institutes of Health) Clinical Laboratory for their help in collecting human samples. We also thank staff members of the Perinatology Research Branch Histology and Pathology Units for examination of pathological sections and Maureen McGerty for critical reading of the manuscript.

Disclosures

The authors have no financial conflicts of interest.

References

1. Liu, L., S. Oza, D. Hogan, J. Perin, I. Rudan, J. E. Lawn, S. Cousens, C. Mathers, and R. E. Black. 2015. Global, regional, and national causes of child mortality in 2000-13, with projections to inform post-2015 priorities: an updated systematic analysis. *Lancet* 385: 430–440.
2. Martin, J. A., B. E. Hamilton, M. J. Osterman, S. C. Curtin, and T. J. Matthews. 2015. Births: final data for 2013. *Natl. Vital Stat. Rep.* 64: 1–65.
3. Lubow, J. M., H. Y. How, M. Habli, R. Maxwell, and B. M. Sibai. 2009. Indications for delivery and short-term neonatal outcomes in late preterm as compared with term births. *Am. J. Obstet. Gynecol.* 200: e30–e33.
4. Mwaniki, M. K., M. Atieno, J. E. Lawn, and C. R. Newton. 2012. Long-term neurodevelopmental outcomes after intrauterine and neonatal insults: a systematic review. *Lancet* 379: 445–452.
5. Manuck, T. A., X. Sheng, B. A. Yoder, and M. W. Varner. 2014. Correlation between initial neonatal and early childhood outcomes following preterm birth. *Am. J. Obstet. Gynecol.* 210: 426.e1–9. doi:10.1016/j.ajog.2014.01.046
6. Behrman R. E., and A. S. Butler, eds. 2007. *Preterm Birth: Causes, Consequences, and Prevention*. National Academies Press, Washington, DC.
7. Blencowe, H., S. Cousens, M. Z. Oestergaard, D. Chou, A. B. Moller, R. Narwal, A. Adler, C. Vera Garcia, S. Rohde, L. Say, and J. E. Lawn. 2012. National, regional, and worldwide estimates of preterm birth rates in the year 2010 with time trends since 1990 for selected countries: a systematic analysis and implications. *Lancet* 379: 2162–2172.
8. Shapiro-Mendoza, C. K., and E. M. Lackritz. 2012. Epidemiology of late and moderate preterm birth. *Semin. Fetal Neonatal Med.* 17: 120–125.
9. Goldenberg, R. L., J. F. Culhane, J. D. Iams, and R. Romero. 2008. Epidemiology and causes of preterm birth. *Lancet* 371: 75–84.
10. Romero, R., S. K. Dey, and S. J. Fisher. 2014. Preterm labor: one syndrome, many causes. *Science* 345: 760–765.
11. Romero, R., M. Sirtori, E. Oyarzun, C. Avila, M. Mazor, R. Callahan, V. Sabo, A. P. Athanassiadis, and J. C. Hobbins. 1989. Infection and labor. V. Prevalence, microbiology, and clinical significance of intraamniotic infection in women with preterm labor and intact membranes. *Am. J. Obstet. Gynecol.* 161: 817–824.
12. Romero, R., C. Avila, U. Santhanam, and P. B. Sehgal. 1990. Amniotic fluid interleukin 6 in preterm labor. Association with infection. *J. Clin. Invest.* 85: 1392–1400.
13. Romero, R., R. Quintero, J. Nores, C. Avila, M. Mazor, S. Hanaoka, Z. Hagay, L. Merchant, and J. C. Hobbins. 1991. Amniotic fluid white blood cell count: a rapid and simple test to diagnose microbial invasion of the amniotic cavity and predict preterm delivery. *Am. J. Obstet. Gynecol.* 165: 821–830.
14. Romero, R., M. Mazor, H. Munoz, R. Gomez, M. Galasso, and D. M. Sherer. 1994. The preterm labor syndrome. *Ann. N. Y. Acad. Sci.* 734: 414–429.
15. Andrews, W. W., J. C. Hauth, R. L. Goldenberg, R. Gomez, R. Romero, and G. H. Cassell. 1995. Amniotic fluid interleukin-6: correlation with upper genital tract microbial colonization and gestational age in women delivered after spontaneous labor versus indicated delivery. *Am. J. Obstet. Gynecol.* 173: 606–612.
16. Yoon, B. H., J. K. Jun, K. H. Park, H. C. Syn, R. Gomez, and R. Romero. 1996. Serum C-reactive protein, white blood cell count, and amniotic fluid white blood cell count in women with preterm premature rupture of membranes. *Obstet. Gynecol.* 88: 1034–1040.
17. Yoon, B. H., J. W. Chang, and R. Romero. 1998. Isolation of *Ureaplasma urealyticum* from the amniotic cavity and adverse outcome in preterm labor. *Obstet. Gynecol.* 92: 77–82.
18. Gomez, R., R. Romero, F. Ghezzi, B. H. Yoon, M. Mazor, and S. M. Berry. 1998. The fetal inflammatory response syndrome. *Am. J. Obstet. Gynecol.* 179: 194–202.
19. Yoon, B. H., R. Romero, M. Kim, E. C. Kim, T. Kim, J. S. Park, and J. K. Jun. 2000. Clinical implications of detection of *Ureaplasma urealyticum* in the amniotic cavity with the polymerase chain reaction. *Am. J. Obstet. Gynecol.* 183: 1130–1137.
20. Romero, R., R. Gómez, T. Chaiworapongsa, G. Conoscenti, J. C. Kim, and Y. M. Kim. 2001. The role of infection in preterm labour and delivery. *Paediatr. Perinat. Epidemiol.* 15(Suppl. 2): 41–56.
21. Yoon, B. H., R. Romero, J. B. Moon, S. S. Shim, M. Kim, G. Kim, and J. K. Jun. 2001. Clinical significance of intra-amniotic inflammation in patients with preterm labor and intact membranes. *Am. J. Obstet. Gynecol.* 185: 1130–1136.
22. Jacobsson, B., I. Mattsby-Baltzer, B. Andersch, H. Bokström, R. M. Holst, U. B. Wennerholm, and H. Hagberg. 2003. Microbial invasion and cytokine response in amniotic fluid in a Swedish population of women in preterm labor. *Acta Obstet. Gynecol. Scand.* 82: 120–128.
23. Shim, S. S., R. Romero, J. S. Hong, C. W. Park, J. K. Jun, B. I. Kim, and B. H. Yoon. 2004. Clinical significance of intra-amniotic inflammation in patients with preterm premature rupture of membranes. *Am. J. Obstet. Gynecol.* 191: 1339–1345.

24. Romero, R., J. Espinoza, L. F. Gonçalves, J. P. Kusanovic, L. Friel, and S. Hassan. 2007. The role of inflammation and infection in preterm birth. *Semin. Reprod. Med.* 25: 21–39.
25. Lee, S. E., R. Romero, H. Jung, C. W. Park, J. S. Park, and B. H. Yoon. 2007. The intensity of the fetal inflammatory response in intraamniotic inflammation with and without microbial invasion of the amniotic cavity. *Am. J. Obstet. Gynecol.* 197: 294.e1–6. doi:10.1016/j.ajog.2007.07.006
26. Kallapur, S. G., B. W. Kramer, C. L. Knox, C. A. Berry, J. J. Collins, M. W. Kemp, I. Nitsos, G. R. Polglase, J. Robinson, N. H. Hillman, et al. 2011. Chronic fetal exposure to *Ureaplasma parvum* suppresses innate immune responses in sheep. *J. Immunol.* 187: 2688–2695.
27. Cobo, T., M. Palacio, M. Martinez-Terron, A. Navarro-Sastre, J. Bosch, X. Filella, and E. Gratacos. 2011. Clinical and inflammatory markers in amniotic fluid as predictors of adverse outcomes in preterm premature rupture of membranes. *Am. J. Obstet. Gynecol.* 205: 126.e1–8. doi:10.1016/j.ajog.2011.03.050
28. Agrawal, V., and E. Hirsch. 2012. Intrauterine infection and preterm labor. *Semin. Fetal Neonatal Med.* 17: 12–19.
29. Romero, R., J. Miranda, T. Chaiworapongsa, P. Chaemsaithong, F. Gotsch, Z. Dong, A. I. Ahmed, B. H. Yoon, S. S. Hassan, C. J. Kim, et al. 2014. Sterile intra-amniotic inflammation in asymptomatic patients with a sonographic short cervix: prevalence and clinical significance. *J. Matern. Fetal Neonatal Med.* Sept. 24: 1–17.
30. Romero, R., J. Miranda, T. Chaiworapongsa, S. J. Korzeniewski, P. Chaemsaithong, F. Gotsch, Z. Dong, A. I. Ahmed, B. H. Yoon, S. S. Hassan, et al. 2014. Prevalence and clinical significance of sterile intra-amniotic inflammation in patients with preterm labor and intact membranes. *Am. J. Reprod. Immunol.* 72: 458–474.
31. Romero, R., J. Miranda, T. Chaiworapongsa, P. Chaemsaithong, F. Gotsch, Z. Dong, A. I. Ahmed, B. H. Yoon, S. S. Hassan, C. J. Kim, et al. 2014. A novel molecular microbiologic technique for the rapid diagnosis of microbial invasion of the amniotic cavity and intra-amniotic infection in preterm labor with intact membranes. *Am. J. Reprod. Immunol.* 71: 330–358.
32. Romero, R., J. Miranda, P. Chaemsaithong, T. Chaiworapongsa, J. P. Kusanovic, Z. Dong, A. I. Ahmed, M. Shaman, K. Lannaman, B. H. Yoon, et al. 2015. Sterile and microbial-associated intra-amniotic inflammation in preterm prelabor rupture of membranes. *J. Matern. Fetal Neonatal Med.* 28: 1394–1409.
33. Combs, C. A., M. Gravett, T. J. Garite, D. E. Hickok, J. Lapidus, R. Porreco, J. Rael, T. Grove, T. K. Morgan, W. Clewell, et al., and ProteoGenix/Obstetrix Collaborative Research Network. 2014. Amniotic fluid infection, inflammation, and colonization in preterm labor with intact membranes. *Am. J. Obstet. Gynecol.* 210: 125.e1–125.e15.
34. Kacerovsky, M., I. Musilova, C. Andrys, H. Hornychova, L. Pliskova, M. Kostal, and B. Jacobsson. 2014. Prelabor rupture of membranes between 34 and 37 weeks: the intraamniotic inflammatory response and neonatal outcomes. *Am. J. Obstet. Gynecol.* 210: 325.e1–325.e10. doi:10.1016/j.ajog.2013.10.882
35. Gervasi, M. T., T. Chaiworapongsa, N. Naccasha, S. Blackwell, B. H. Yoon, E. Maymon, and R. Romero. 2001. Phenotypic and metabolic characteristics of maternal monocytes and granulocytes in preterm labor with intact membranes. *Am. J. Obstet. Gynecol.* 185: 1124–1129.
36. Gervasi, M. T., T. Chaiworapongsa, N. Naccasha, P. Pacora, S. Berman, E. Maymon, J. C. Kim, Y. M. Kim, J. Yoshimatsu, J. Espinoza, and R. Romero. 2002. Maternal intravascular inflammation in preterm premature rupture of membranes. *J. Matern. Fetal Neonatal Med.* 11: 171–175.
37. Mittal, P., R. Romero, A. L. Tarca, S. Draghici, C. L. Nhan-Chang, T. Chaiworapongsa, J. Hotra, R. Gomez, J. P. Kusanovic, D. C. Lee, et al. 2011. A molecular signature of an arrest of descent in human parturition. *Am. J. Obstet. Gynecol.* 204: 177.e15–33.doi:10.1016/j.ajog.2010.09.025
38. Chaemsaithong, P., I. Madan, R. Romero, N. G. Than, A. L. Tarca, S. Draghici, G. Bhatti, L. Yeo, M. Mazor, C. J. Kim, et al. 2013. Characterization of the myometrial transcriptome in women with an arrest of dilatation during labor. *J. Perinat. Med.* 41: 665–681.
39. Kim, Y. M., R. Romero, T. Chaiworapongsa, G. J. Kim, M. R. Kim, H. Kuivaniemi, G. Tromp, J. Espinoza, E. Bujold, V. M. Abrahams, and G. Mor. 2004. Toll-like receptor-2 and -4 in the chorioamniotic membranes in spontaneous labor at term and in preterm parturition that are associated with chorioamnionitis. *Am. J. Obstet. Gynecol.* 191: 1346–1355.
40. Murphy, S. P., N. N. Hanna, L. D. Fast, S. K. Shaw, G. Berg, J. F. Padbury, R. Romero, and S. Sharma. 2009. Evidence for participation of uterine natural killer cells in the mechanisms responsible for spontaneous preterm labor and delivery. *Am. J. Obstet. Gynecol.* 200: 308.e1–9.doi:10.1016/j.ajog.2008.10.043
41. Koga, K., I. Cardenas, P. Aldo, V. M. Abrahams, B. Peng, S. Fill, R. Romero, and G. Mor. 2009. Activation of TLR3 in the trophoblast is associated with preterm delivery. *Am. J. Reprod. Immunol.* 61: 196–212.
42. Cardenas, I., R. E. Means, P. Aldo, K. Koga, S. M. Lang, C. J. Booth, A. Manzur, E. Oyarzun, R. Romero, and G. Mor. 2010. Viral infection of the placenta leads to fetal inflammation and sensitization to bacterial products predisposing to preterm labor. *J. Immunol.* 185: 1248–1257.
43. Cardenas, I., M. J. Mulla, K. Myrtolli, A. K. Sfakianaki, E. R. Norwitz, S. Tadesse, S. Guller, and V. M. Abrahams. 2011. Nod1 activation by bacterial iE-DAP induces maternal-fetal inflammation and preterm labor. *J. Immunol.* 187: 980–986.
44. Romero, R., T. Chaiworapongsa, Z. Alpay Savasan, Y. Xu, Y. Hussein, Z. Dong, J. P. Kusanovic, C. J. Kim, and S. S. Hassan. 2011. Damage-associated molecular patterns (DAMPs) in preterm labor with intact membranes and preterm PROM: a study of the alarmin HMGB1. *J. Matern. Fetal Neonatal Med.* 24: 1444–1455.
45. Jaiswal, M. K., V. Agrawal, T. Mallers, A. Gilman-Sachs, E. Hirsch, and K. D. Beaman. 2013. Regulation of apoptosis and innate immune stimuli in inflammation-induced preterm labor. *J. Immunol.* 191: 5702–5713.
46. Shynlova, O., T. Nedd-Roderique, Y. Li, A. Dorogin, and S. J. Lye. 2013. Myometrial immune cells contribute to term parturition, preterm labour and post-partum involution in mice. *J. Cell. Mol. Med.* 17: 90–102.
47. Arenas-Hernandez, M., R. Romero, D. St Louis, S. S. Hassan, E. B. Kaye, and N. Gomez-Lopez. 2015. An imbalance between innate and adaptive immune cells at the maternal-fetal interface occurs prior to endotoxin-induced preterm birth. *Cell. Mol. Immunol.* DOI: 10.1038/cmi.2015.22.
48. Thaxton, J. E., T. A. Nevers, and S. Sharma. 2010. TLR-mediated preterm birth in response to pathogenic agents. *Infect. Dis. Obstet. Gynecol.* 2010: 2010.
49. Friel, L. A., R. Romero, S. Edwin, J. K. Nien, R. Gomez, T. Chaiworapongsa, J. P. Kusanovic, J. E. Tolosa, S. S. Hassan, and J. Espinoza. 2007. The calcium binding protein, S100B, is increased in the amniotic fluid of women with intra-amniotic infection/inflammation and preterm labor with intact or ruptured membranes. *J. Perinat. Med.* 35: 385–393.
50. Romero, R., J. Espinoza, S. Hassan, F. Gotsch, J. P. Kusanovic, C. Avila, O. Erez, S. Edwin, and A. M. Schmidt. 2008. Soluble receptor for advanced glycation end products (sRAGE) and endogenous secretory RAGE (esRAGE) in amniotic fluid: modulation by infection and inflammation. *J. Perinat. Med.* 36: 388–398.
51. Chaiworapongsa, T., O. Erez, J. P. Kusanovic, E. Vaisbuch, S. Mazaki-Tovi, F. Gotsch, N. G. Than, P. Mittal, Y. M. Kim, N. Camacho, et al. 2008. Amniotic fluid heat shock protein 70 concentration in histologic chorioamnionitis, term and preterm parturition. *J. Matern. Fetal Neonatal Med.* 21: 449–461.
52. Lee, S. E., I. S. Park, R. Romero, and B. H. Yoon. 2009. Amniotic fluid prostaglandin F2 increases even in sterile amniotic fluid and is an independent predictor of impending delivery in preterm premature rupture of membranes. *J. Matern. Fetal Neonatal Med.* 22: 880–886.
53. Lotze, M. T., A. Deisseroth, and A. Rubartelli. 2007. Damage associated molecular pattern molecules. *Clin. Immunol.* 124: 1–4.
54. Oppenheim, J. J., and D. Yang. 2005. Alarmins: chemotactic activators of immune responses. *Curr. Opin. Immunol.* 17: 359–365.
55. Chen, G. Y., and G. Nuñez. 2010. Sterile inflammation: sensing and reacting to damage. *Nat. Rev. Immunol.* 10: 826–837.
56. Espinoza, J., R. Romero, T. Chaiworapongsa, J. C. Kim, J. Yoshimatsu, S. Edwin, C. Rathnasabapathy, J. Tolosa, A. Donnenfeld, F. Craparo, et al. 2002. Lipopolysaccharide-binding protein in microbial invasion of the amniotic cavity and human parturition. *J. Matern. Fetal Neonatal Med.* 12: 313–321.
57. Romero, R., J. Miranda, P. Chaemsaithong, T. Chaiworapongsa, J. P. Kusanovic, Z. Dong, A. I. Ahmed, M. Shaman, K. Lannaman, B. H. Yoon, et al. 2015. Sterile and microbial-associated intra-amniotic inflammation in preterm prelabor rupture of membranes. *J. Matern. Fetal Neonatal Med.* 28: 1394–1409.
58. Romero, R., M. Mazor, and B. Tartakovsky. 1991. Systemic administration of interleukin-1 induces preterm parturition in mice. *Am. J. Obstet. Gynecol.* 165: 969–971.
59. Gomez-Lopez, N., R. Romero, O. Plazyo, B. Panaitescu, A. E. Furcron, D. Miller, T. Roumayah, E. Flom, and S. A. Hassan. 2016. Intra-amniotic administration of HMGB1 induces spontaneous preterm labor and birth. *Am. J. Reprod. Immunol.* In press.
60. Cayrol, C., and J. P. Girard. 2009. The IL-1-like cytokine IL-33 is inactivated after maturation by caspase-1. *Proc. Natl. Acad. Sci. USA* 106: 9021–9026.
61. Topping, V., R. Romero, N. G. Than, A. L. Tarca, Z. Xu, S. Y. Kim, B. Wang, L. Yeo, C. J. Kim, S. S. Hassan, and J. S. Kim. 2013. Interleukin-33 in the human placenta. *J. Matern. Fetal Neonatal Med.* 26: 327–338.
62. Kim, C. J., R. Romero, P. Chaemsaithong, N. Chaiyasit, B. H. Yoon, and Y. M. Kim. 2015. Acute chorioamnionitis and funisitis: definition, pathologic features, and clinical significance. *Am. J. Obstet. Gynecol.* 213(4, Suppl.)S29–S52.
63. Bourgeois, E., L. P. Van, M. Samson, S. Diem, A. Barra, S. Roga, J. M. Gombert, E. Schneider, M. Dy, P. Gourdy, et al. 2009. The pro-Th2 cytokine IL-33 directly interacts with invariant NKT and NK cells to induce IFN-gamma production. *Eur. J. Immunol.* 39: 1046–1055.
64. Smithgall, M. D., M. R. Comeau, B. R. Yoon, D. Kaufman, R. Armitage, and D. E. Smith. 2008. IL-33 amplifies both Th1- and Th2-type responses through its activity on human basophils, allergen-reactive Th2 cells, iNKT and NK cells. *Int. Immunol.* 20: 1019–1030.
65. Kitamura, H., K. Iwakabe, T. Yahata, S. Nishimura, A. Ohta, Y. Ohmi, M. Sato, K. Takeda, K. Okumura, L. Van Kaer, et al. 1999. The natural killer T (NKT) cell ligand alpha-galactosylceramide demonstrates its immunopotentiating effect by inducing interleukin (IL)-12 production by dendritic cells and IL-12 receptor expression on NKT cells. *J. Exp. Med.* 189: 1121–1128.
66. Tomura, M., W. G. Yu, H. J. Ahn, M. Yamashita, Y. F. Yang, S. Ono, T. Hamaoka, T. Kawano, M. Taniguchi, Y. Koezuka, and H. Fujiwara. 1999. A novel function of Valpha14+CD4+NKT cells: stimulation of IL-12 production by antigen-presenting cells in the innate immune system. *J. Immunol.* 163: 93–101.
67. Fujii, S., K. Shimizu, M. Kronenberg, and R. M. Steinman. 2002. Prolonged IFN-gamma-producing NKT response induced with alpha-galactosylceramide-loaded DCs. *Nat. Immunol.* 3: 867–874.
68. Brigl, M., L. Bry, S. C. Kent, J. E. Gumperz, and M. B. Brenner. 2003. Mechanism of CD1d-restricted natural killer T cell activation during microbial infection. *Nat. Immunol.* 4: 1230–1237.
69. Oki, S., A. Chiba, T. Yamamura, and S. Miyake. 2004. The clinical implication and molecular mechanism of preferential IL-4 production by modified glycolipid-stimulated NKT cells. *J. Clin. Invest.* 113: 1631–1640.

70. Sag, D., P. Krause, C. C. Hedrick, M. Kronenberg, and G. Wingender. 2014. IL-10-producing NKT10 cells are a distinct regulatory invariant NKT cell subset. *J. Clin. Invest.* 124: 3725–3740.
71. Bendelac, A., P. B. Savage, and L. Teyton. 2007. The biology of NKT cells. *Annu. Rev. Immunol.* 25: 297–336.
72. Kawano, T., J. Cui, Y. Koezuka, I. Toura, Y. Kaneko, K. Motoki, H. Ueno, R. Nakagawa, H. Sato, E. Kondo, et al. 1997. CD1d-restricted and TCR-mediated activation of valpha14 NKT cells by glycosylceramides. *Science* 278: 1626–1629.
73. Sidobre, S., O. V. Naidenko, B. C. Sim, N. R. Gascoigne, K. C. Garcia, and M. Kronenberg. 2002. The V alpha 14 NKT cell TCR exhibits high-affinity binding to a glycolipid/CD1d complex. *J. Immunol.* 169: 1340–1348.
74. Lehmann, J. M., L. B. Moore, T. A. Smith-Oliver, W. O. Wilkison, T. M. Willson, and S. A. Kliewer. 1995. An antidiabetic thiazolidinedione is a high affinity ligand for peroxisome proliferator-activated receptor gamma (PPAR gamma). *J. Biol. Chem.* 270: 12953–12956.
75. Ricote, M., A. C. Li, T. M. Willson, C. J. Kelly, and C. K. Glass. 1998. The peroxisome proliferator-activated receptor-gamma is a negative regulator of macrophage activation. *Nature* 391: 79–82.
76. Chinetti, G., S. Griglio, M. Antonucci, I. P. Torra, P. Delerive, Z. Majd, J. C. Fruchart, J. Chapman, J. Najib, and B. Staels. 1998. Activation of proliferator-activated receptors alpha and gamma induces apoptosis of human monocyte-derived macrophages. *J. Biol. Chem.* 273: 25573–25580.
77. Delerive, P., F. Martin-Nizard, G. Chinetti, F. Trottein, J. C. Fruchart, J. Najib, P. Duriez, and B. Staels. 1999. Peroxisome proliferator-activated receptor activators inhibit thrombin-induced endothelin-1 production in human vascular endothelial cells by inhibiting the activator protein-1 signaling pathway. *Circ. Res.* 85: 394–402.
78. McCarthy, F. P., A. C. Delany, L. C. Kenny, and S. K. Walsh. 2013. PPAR-γ – a possible drug target for complicated pregnancies. *Br. J. Pharmacol.* 168: 1074–1085.
79. Forman, B. M., P. Tontonoz, J. Chen, R. P. Brun, B. M. Spiegelman, and R. M. Evans. 1995. 15-Deoxy-delta 12, 14-prostaglandin J2 is a ligand for the adipocyte determination factor PPAR gamma. *Cell* 83: 803–812.
80. Kliewer, S. A., J. M. Lenhard, T. M. Willson, I. Patel, D. C. Morris, and J. M. Lehmann. 1995. A prostaglandin J2 metabolite binds peroxisome proliferator-activated receptor gamma and promotes adipocyte differentiation. *Cell* 83: 813–819.
81. Pirianov, G., S. N. Waddington, T. M. Lindström, V. Terzidou, H. Mehmet, and P. R. Bennett. 2009. The cyclopentenone 15-deoxy-delta 12,14-prostaglandin J(2) delays lipopolysaccharide-induced preterm delivery and reduces mortality in the newborn mouse. *Endocrinology* 150: 699–706.
82. Arenas-Hernandez, M., E. N. Sanchez-Rodriguez, T. N. Mial, S. A. Robertson, and N. Gomez-Lopez. 2015. Isolation of leukocytes from the murine tissues at the maternal-fetal interface. *J. Vis. Exp.* 99: e52866.
83. American College of Obstetrics and Gynecology Committee on Practice Bulletins-Obstetrics. 2003. ACOG Practice Bulletin Number 49, December 2003: Dystocia and augmentation of labor. *Obstet. Gynecol.* 102: 1445–1454.
84. Redline, R. W. 2008. Placental pathology: a systematic approach with clinical correlations. *Placenta* 29 Suppl. A: S86–91. doi:10.1016/j.placenta.2007.09.003
85. Kim, C. J., R. Romero, J. P. Kusanovic, W. Yoo, Z. Dong, V. Topping, F. Gotsch, B. H. Yoon, J. G. Chi, and J. S. Kim. 2010. The frequency, clinical significance, and pathological features of chronic chorioamnionitis: a lesion associated with spontaneous preterm birth. *Mod. Pathol.* 23: 1000–1011.
86. Xu, Y., O. Plazyo, R. Romero, S. S. Hassan, and N. Gomez-Lopez. 2015. Isolation of leukocytes from the human maternal-fetal interface. *J. Vis. Exp.* 99: e52863.
87. Rochelson, B. L., H. Schulman, A. Fleischer, G. Farmakides, L. Bracero, J. Ducey, D. Winter, and B. Penny. 1987. The clinical significance of Doppler umbilical artery velocimetry in the small for gestational age fetus. *Am. J. Obstet. Gynecol.* 156: 1223–1226.
88. Schulman, H. 1987. The clinical implications of Doppler ultrasound analysis of the uterine and umbilical arteries. *Am. J. Obstet. Gynecol.* 156: 889–893.
89. 1995. ACOG technical bulletin. Fetal heart rate patterns: monitoring, interpretation, and management. Number 207–July 1995 (replaces No. 132, September 1989). *Int. J. Gynaecol. Obstet.* 51: 65–74.
90. The National Institute of Child Health and Human Development Research Planning Workshop. 1997. Electronic fetal heart rate monitoring: research guidelines for interpretation. *J. Obstet. Gynecol. Neonatal Nurs.* 26: 635–640.
91. Boyson, J. E., N. Nagarkatti, L. Nizam, M. A. Exley, and J. L. Strominger. 2006. Gestation stage-dependent mechanisms of invariant natural killer T cell-mediated pregnancy loss. *Proc. Natl. Acad. Sci. USA* 103: 4580–4585.
92. Ito, K., M. Karasawa, T. Kawano, T. Akasaka, H. Koseki, Y. Akutsu, E. Kondo, S. Sekiya, K. Sekikawa, M. Harada, et al. 2000. Involvement of decidual Valpha14 NKT cells in abortion. *Proc. Natl. Acad. Sci. USA* 97: 740–744.
93. Szatmari, I., P. Gogolak, J. S. Im, B. Dezso, E. Rajnavolgyi, and L. Nagy. 2004. Activation of PPARgamma specifies a dendritic cell subtype capable of enhanced induction of iNKT cell expansion. *Immunity* 21: 95–106.
94. Frohnert, B. I., T. Y. Hui, and D. A. Bernlohr. 1999. Identification of a functional peroxisome proliferator-responsive element in the murine fatty acid transport protein gene. *J. Biol. Chem.* 274: 3970–3977.
95. Chiu, Y. H., J. Jayawardena, A. Weiss, D. Lee, S. H. Park, A. Dautry-Varsat, and A. Bendelac. 1999. Distinct subsets of CD1d-restricted T cells recognize self-antigens loaded in different cellular compartments. *J. Exp. Med.* 189: 103–110.
96. Crowe, N. Y., J. M. Coquet, S. P. Berzins, K. Kyparissoudis, R. Keating, D. G. Pellicci, Y. Hayakawa, D. I. Godfrey, and M. J. Smyth. 2005. Differential antitumor immunity mediated by NKT cell subsets in vivo. *J. Exp. Med.* 202: 1279–1288.
97. Terabe, M., J. Swann, E. Ambrosino, P. Sinha, S. Takaku, Y. Hayakawa, D. I. Godfrey, S. Ostrand-Rosenberg, M. J. Smyth, and J. A. Berzofsky. 2005. A nonclassical non-Valpha14Jalpha18 CD1d-restricted (type II) NKT cell is sufficient for down-regulation of tumor immunosurveillance. *J. Exp. Med.* 202: 1627–1633.
98. Zheng, Q., L. Zhou, and Q. S. Mi. 2012. MicroRNA miR-150 is involved in Vα14 invariant NKT cell development and function. *J. Immunol.* 188: 2118–2126.
99. Taniguchi, M., K. Seino, and T. Nakayama. 2003. The NKT cell system: bridging innate and acquired immunity. *Nat. Immunol.* 4: 1164–1165.
100. Carnaud, C., D. Lee, O. Donnars, S. H. Park, A. Beavis, Y. Koezuka, and A. Bendelac. 1999. Cutting edge: Cross-talk between cells of the innate immune system: NKT cells rapidly activate NK cells. *J. Immunol.* 163: 4647–4650.
101. Singh, N., S. Hong, D. C. Scherer, I. Serizawa, N. Burdin, M. Kronenberg, Y. Koezuka, and L. Van Kaer. 1999. Cutting edge: activation of NK T cells by CD1d and alpha-galactosylceramide directs conventional T cells to the acquisition of a Th2 phenotype. *J. Immunol.* 163: 2373–2377.
102. Nishimura, T., H. Kitamura, K. Iwakabe, T. Yahata, A. Ohta, M. Sato, K. Takeda, K. Okumura, L. Van Kaer, T. Kawano, et al. 2000. The interface between innate and acquired immunity: glycolipid antigen presentation by CD1d-expressing dendritic cells to NKT cells induces the differentiation of antigen-specific cytotoxic T lymphocytes. *Int. Immunol.* 12: 987–994.
103. Kitamura, H., A. Ohta, M. Sekimoto, M. Sato, K. Iwakabe, M. Nakui, T. Yahata, H. Meng, T. Koda, S. Nishimura, et al. 2000. alpha-galactosylceramide induces early B-cell activation through IL-4 production by NKT cells. *Cell. Immunol.* 199: 37–42.
104. Wang, H., D. Feng, O. Park, S. Yin, and B. Gao. 2013. Invariant NKT cell activation induces neutrophil accumulation and hepatitis: opposite regulation by IL-4 and IFN-γ. *Hepatology* 58: 1474–1485.
105. Fujii, S., K. Shimizu, C. Smith, L. Bonifaz, and R. M. Steinman. 2003. Activation of natural killer T cells by alpha-galactosylceramide rapidly induces the full maturation of dendritic cells in vivo and thereby acts as an adjuvant for combined CD4 and CD8 T cell immunity to a coadministered protein. *J. Exp. Med.* 198: 267–279.
106. Xue, J., S. V. Schmidt, J. Sander, A. Draffehn, W. Krebs, I. Quester, D. De Nardo, T. D. Gohel, M. Emde, L. Schmidleithner, et al. 2014. Transcriptome-based network analysis reveals a spectrum model of human macrophage activation. *Immunity* 40: 274–288.
107. Murray, P. J., J. E. Allen, S. K. Biswas, E. A. Fisher, D. W. Gilroy, S. Goerdt, S. Gordon, J. A. Hamilton, L. B. Ivashkiv, T. Lawrence, et al. 2014. Macrophage activation and polarization: nomenclature and experimental guidelines. *Immunity* 41: 14–20.
108. Mills, C. D., K. Kincaid, J. M. Alt, M. J. Heilman, and A. M. Hill. 2000. M-1/M-2 macrophages and the Th1/Th2 paradigm. *J. Immunol.* 164: 6166–6173.
109. Mantovani, A., S. Sozzani, M. Locati, P. Allavena, and A. Sica. 2002. Macrophage polarization: tumor-associated macrophages as a paradigm for polarized M2 mononuclear phagocytes. *Trends Immunol.* 23: 549–555.
110. Biswas, S. K., and A. Mantovani. 2010. Macrophage plasticity and interaction with lymphocyte subsets: cancer as a paradigm. *Nat. Immunol.* 11: 889–896.
111. Sica, A., and A. Mantovani. 2012. Macrophage plasticity and polarization: in vivo veritas. *J. Clin. Invest.* 122: 787–795.
112. Ellis, T. N., and B. L. Beaman. 2002. Murine polymorphonuclear neutrophils produce interferon-gamma in response to pulmonary infection with *Nocardia asteroides*. *J. Leukoc. Biol.* 72: 373–381.
113. Ethuin, F., B. Gérard, J. E. Benna, A. Boutten, M. A. Gougereot-Pocidalo, L. Jacob, and S. Chollet-Martin. 2004. Human neutrophils produce interferon gamma upon stimulation by interleukin-12. *Lab. Invest.* 84: 1363–1371.
114. Boyson, J. E., B. Rybalov, L. A. Koopman, M. Exley, S. P. Balk, F. K. Racke, F. Schatz, R. Masch, S. B. Wilson, and J. L. Strominger. 2002. CD1d and invariant NKT cells at the human maternal-fetal interface. *Proc. Natl. Acad. Sci. USA* 99: 13741–13746.
115. Li, L. P., Y. C. Fang, G. F. Dong, Y. Lin, and S. Saito. 2012. Depletion of invariant NKT cells reduces inflammation-induced preterm delivery in mice. *J. Immunol.* 188: 4681–4689.
116. Li, L., J. Yang, Y. Jiang, J. Tu, and D. J. Schust. 2015. Activation of decidual invariant natural killer T cells promotes lipopolysaccharide-induced preterm birth. *Mol. Hum. Reprod.* 21: 369–381.
117. Mattner, J., K. L. Debord, N. Ismail, R. D. Goff, C. Cantu, III, D. Zhou, P. Saint-Mezard, V. Wang, Y. Gao, N. Yin, et al. 2005. Exogenous and endogenous glycolipid antigens activate NKT cells during microbial infections. *Nature* 434: 525–529.
118. Aluvihare, V. R., M. Kallikourdis, and A. G. Betz. 2004. Regulatory T cells mediate maternal tolerance to the fetus. *Nat. Immunol.* 5: 266–271.
119. Rowe, J. H., J. M. Ertelt, L. Xin, and S. S. Way. 2012. Pregnancy imprints regulatory memory that sustains anergy to fetal antigen. *Nature* 490: 102–106.
120. Shima, T., Y. Sasaki, M. Itoh, A. Nakashima, N. Ishii, K. Sugamura, and S. Saito. 2010. Regulatory T cells are necessary for implantation and maintenance of early pregnancy but not late pregnancy in allogeneic mice. *J. Reprod. Immunol.* 85: 121–129.
121. Wang, M. L., D. J. Dorer, M. P. Fleming, and E. A. Catlin. 2004. Clinical outcomes of near-term infants. *Pediatrics* 114: 372–376.

122. Raju, T. N., R. D. Higgins, A. R. Stark, and K. J. Leveno. 2006. Optimizing care and outcome for late-preterm (near-term) infants: a summary of the workshop sponsored by the National Institute of Child Health and Human Development. *Pediatrics* 118: 1207–1214.
123. Pellicci, D. G., K. J. Hammond, A. P. Uldrich, A. G. Baxter, M. J. Smyth, and D. I. Godfrey. 2002. A natural killer T (NKT) cell developmental pathway iInvolving a thymus-dependent NK1.1(−)CD4(+) CD1d-dependent precursor stage. *J. Exp. Med.* 195: 835–844.
124. Dunn-Albanese, L. R., W. E. Ackerman, IV, Y. Xie, J. D. Iams, and D. A. Kniss. 2004. Reciprocal expression of peroxisome proliferator-activated receptor-gamma and cyclooxygenase-2 in human term parturition. *Am. J. Obstet. Gynecol.* 190: 809–816.
125. Mial, N. T., L. Kadam, R. Romero, S. Drewlo, and N. Gomez-Lopez. 2015. Rosiglitazone treatment rapidly controls the systemic pro-inflammatory response and reduces the rate of infection-induced preterm birth. *Reprod. Sci.* 22: 137A (Abstr.).
126. Crowe, N. Y., A. P. Uldrich, K. Kyparissoudis, K. J. Hammond, Y. Hayakawa, S. Sidobre, R. Keating, M. Kronenberg, M. J. Smyth, and D. I. Godfrey. 2003. Glycolipid antigen drives rapid expansion and sustained cytokine production by NK T cells. *J. Immunol.* 171: 4020–4027.
127. Szatmari, I., A. Pap, R. Rühl, J. X. Ma, P. A. Illarionov, G. S. Besra, E. Rajnavolgyi, B. Dezso, and L. Nagy. 2006. PPARgamma controls CD1d expression by turning on retinoic acid synthesis in developing human dendritic cells. *J. Exp. Med.* 203: 2351–2362.
128. Brossay, L., D. Jullien, S. Cardell, B. C. Sydora, N. Burdin, R. L. Modlin, and M. Kronenberg. 1997. Mouse CD1 is mainly expressed on hemopoietic-derived cells. *J. Immunol.* 159: 1216–1224.
129. Roark, J. H., S. H. Park, J. Jayawardena, U. Kavita, M. Shannon, and A. Bendelac. 1998. CD1.1 expression by mouse antigen-presenting cells and marginal zone B cells. *J. Immunol.* 160: 3121–3127.
130. Bendelac, A. 1995. Positive selection of mouse NK1+ T cells by CD1-expressing cortical thymocytes. *J. Exp. Med.* 182: 2091–2096.
131. Gomez-Lopez, N., L. J. Guilbert, and D. M. Olson. 2010. Invasion of the leukocytes into the fetal-maternal interface during pregnancy. *J. Leukoc. Biol.* 88: 625–633.
132. Gomez-Lopez, N., D. StLouis, M. A. Lehr, E. N. Sanchez-Rodriguez, and M. Arenas-Hernandez. 2014. Immune cells in term and preterm labor. *Cell. Mol. Immunol.* 11: 571–581.
133. Bizargity, P., R. Del Rio, M. Phillippe, C. Teuscher, and E. A. Bonney. 2009. Resistance to lipopolysaccharide-induced preterm delivery mediated by regulatory T cell function in mice. *Biol. Reprod.* 80: 874–881.
134. Gomez-Lopez, N., L. Vadillo-Perez, A. Hernandez-Carbajal, M. Godines-Enriquez, D. M. Olson, and F. Vadillo-Ortega. 2011. Specific inflammatory microenvironments in the zones of the fetal membranes at term delivery. *Am. J. Obstet. Gynecol.* 205: 235.e15–24. doi:10.1016/j.ajog.2011.04.019
135. Gomez-Lopez, N., R. Vega-Sanchez, M. Castillo-Castrejon, R. Romero, K. Cubeiro-Arreola, and F. Vadillo-Ortega. 2013. Evidence for a role for the adaptive immune response in human term parturition. *Am. J. Reprod. Immunol.* 69: 212–230.
136. Gomez-Lopez, N., D. M. Olson, and S. A. Robertson. 2015. Interleukin-6 controls uterine Th9 cells and CD8 T regulatory cells to accelerate parturition in mice. *Immunol. Cell Biol*. DOI: 10.1038/icb.2015.63.
137. Marx, N., B. Kehrle, K. Kohlhammer, M. Grüb, W. Koenig, V. Hombach, P. Libby, and J. Plutzky. 2002. PPAR activators as antiinflammatory mediators in human T lymphocytes: implications for atherosclerosis and transplantation-associated arteriosclerosis. *Circ. Res.* 90: 703–710.
138. Yang, X. Y., L. H. Wang, T. Chen, D. R. Hodge, J. H. Resau, L. DaSilva, and W. L. Farrar. 2000. Activation of human T lymphocytes is inhibited by peroxisome proliferator-activated receptor gamma (PPARgamma) agonists. PPARgamma co-association with transcription factor NFAT. *J. Biol. Chem.* 275: 4541–4544.
139. Gonzalez, J. M., C. W. Franzke, F. Yang, R. Romero, and G. Girardi. 2011. Complement activation triggers metalloproteinases release inducing cervical remodeling and preterm birth in mice. *Am. J. Pathol.* 179: 838–849.
140. Jiang, C., A. T. Ting, and B. Seed. 1998. PPAR-gamma agonists inhibit production of monocyte inflammatory cytokines. *Nature* 391: 82–86.
141. Kintscher, U., S. Goetze, S. Wakino, S. Kim, S. Nagpal, R. A. Chandraratna, K. Graf, E. Fleck, W. A. Hsueh, and R. E. Law. 2000. Peroxisome proliferator-activated receptor and retinoid X receptor ligands inhibit monocyte chemotactic protein-1-directed migration of monocytes. *Eur. J. Pharmacol.* 401: 259–270.
142. Rinaldi, S. F., R. D. Catalano, J. Wade, A. G. Rossi, and J. E. Norman. 2014. Decidual neutrophil infiltration is not required for preterm birth in a mouse model of infection-induced preterm labor. *J. Immunol.* 192: 2315–2325.
143. Reddy, R. C., V. R. Narala, V. G. Keshamouni, J. E. Milam, M. W. Newstead, and T. J. Standiford. 2008. Sepsis-induced inhibition of neutrophil chemotaxis is mediated by activation of peroxisome proliferator-activated receptor-gamma. *Blood* 112: 4250–4258.
144. Blois, S. M., C. D. Alba Soto, M. Tometten, B. F. Klapp, R. A. Margni, and P. C. Arck. 2004. Lineage, maturity, and phenotype of uterine murine dendritic cells throughout gestation indicate a protective role in maintaining pregnancy. *Biol. Reprod.* 70: 1018–1023.
145. Bizargity, P., and E. A. Bonney. 2009. Dendritic cells: a family portrait at mid-gestation. *Immunology* 126: 565–578.
146. Faveeuw, C., S. Fougeray, V. Angeli, J. Fontaine, G. Chinetti, P. Gosset, P. Delerive, C. Maliszewski, M. Capron, B. Staels, et al. 2000. Peroxisome proliferator-activated receptor gamma activators inhibit interleukin-12 production in murine dendritic cells. *FEBS Lett.* 486: 261–266.
147. Romero, R., K. R. Manogue, M. D. Mitchell, Y. K. Wu, E. Oyarzun, J. C. Hobbins, and A. Cerami. 1989. Infection and labor. IV. Cachectin-tumor necrosis factor in the amniotic fluid of women with intraamniotic infection and preterm labor. *Am. J. Obstet. Gynecol.* 161: 336–341.
148. Casey, M. L., S. M. Cox, B. Beutler, L. Milewich, and P. C. MacDonald. 1989. Cachectin/tumor necrosis factor-alpha formation in human decidua. Potential role of cytokines in infection-induced preterm labor. *J. Clin. Invest.* 83: 430–436.
149. Romero, R., M. Mazor, W. Sepulveda, C. Avila, D. Copeland, and J. Williams. 1992. Tumor necrosis factor in preterm and term labor. *Am. J. Obstet. Gynecol.* 166: 1576–1587.
150. Jacobsson, B., R. M. Holst, U. B. Wennerholm, B. Andersson, H. Lilja, and H. Hagberg. 2003. Monocyte chemotactic protein-1 in cervical and amniotic fluid: relationship to microbial invasion of the amniotic cavity, intra-amniotic inflammation, and preterm delivery. *Am. J. Obstet. Gynecol.* 189: 1161–1167.
151. Esplin, M. S., M. R. Peltier, S. Hamblin, S. Smith, M. B. Fausett, G. A. Dildy, D. W. Branch, R. M. Silver, and E. Y. Adashi. 2005. Monocyte chemotactic protein-1 expression is increased in human gestational tissues during term and preterm labor. *Placenta* 26: 661–671.
152. Esplin, M. S., R. Romero, T. Chaiworapongsa, Y. M. Kim, S. Edwin, R. Gomez, M. Mazor, and E. Y. Adashi. 2005. Monocyte chemotactic protein-1 is increased in the amniotic fluid of women who deliver preterm in the presence or absence of intra-amniotic infection. *J. Matern. Fetal Neonatal Med.* 17: 365–373.
153. Törnblom, S. A., A. Klimaviciute, B. Byström, M. Chromek, A. Brauner, and G. Ekman-Ordeberg. 2005. Non-infected preterm parturition is related to increased concentrations of IL-6, IL-8 and MCP-1 in human cervix. *Reprod. Biol. Endocrinol.* 3: 39.
154. Shynlova, O., P. Tsui, A. Dorogin, and S. J. Lye. 2008. Monocyte chemoattractant protein-1 (CCL-2) integrates mechanical and endocrine signals that mediate term and preterm labor. *J. Immunol.* 181: 1470–1479.
155. Romero, R., J. C. Grivel, A. L. Tarca, P. Chaemsaithong, Z. Xu, W. Fitzgerald, S. S. Hassan, T. Chaiworapongsa, and L. Margolis. 2015. Evidence of perturbations of the cytokine network in preterm labor. *Am. J. Obstet. Gynecol.* July 29. pii: S0002-9378(15)00787-5.
156. Lappas, M., M. Permezel, H. M. Georgiou, and G. E. Rice. 2002. Regulation of proinflammatory cytokines in human gestational tissues by peroxisome proliferator-activated receptor-gamma: effect of 15-deoxy-Delta(12,14)-PGJ(2) and troglitazone. *J. Clin. Endocrinol. Metab.* 87: 4667–4672.
157. Meier, C. A., R. Chicheportiche, C. E. Juge-Aubry, M. G. Dreyer, and J. M. Dayer. 2002. Regulation of the interleukin-1 receptor antagonist in THP-1 cells by ligands of the peroxisome proliferator-activated receptor gamma. *Cytokine* 18: 320–328.